Thermal effects on the spin-domain phases of high spin-f Bose-Einstein condensates with rotational symmetries

Eduardo Serrano-Ensástiga [1,2,*] and Francisco Mireles [1,†]

[1] *Departamento de Física, Centro de Nanociencias y Nanotecnología, Universidad Nacional Autónoma de México Apartado Postal 14, 22800, Ensenada, Baja California, México*

[2] *Institut de Physique Nucléaire, Atomique et de Spectroscopie, CESAM, University of Liège B-4000 Liège, Belgium*

(Received 22 February 2023; accepted 23 October 2023; published 9 November 2023)

In spinor Bose Einstein condensates (BEC) gases, a fraction of its thermally excited atoms can still interact with the condensate ground state, leading to spin-spin interactions that can modify the main features of its spin-phase diagrams. In this work we study the spin-phase diagram of a BEC of general spin-f and fully characterize its noncondensate thermal fraction. The latter provided that the condensate ground state lies within a spin phase with rotational symmetry. The study is based in the Hartree-Fock approximation in conjunction with the Majorana stellar representation approach for pure and mixed quantum states and the use of point-group symmetry arguments. The method allows us to study the phase diagram of spinorial BECs with usual point-group symmetries, including those with some exotic phases associated to the platonic solids ($f = 2, 3, 4$, and 6), which are known to lead to non-Abelian topological excitations. In addition, we explore the temperature effects on the admissible spin-phase domains for general spin values, as well as its physical implications on their multipolar magnetic moments.

DOI: 10.1103/PhysRevA.108.053308

I. INTRODUCTION

Interacting many-body systems with internal spin degrees of freedom, such as unconventional superconductors, helium-3 superfluids, and ultracold atoms, constitute prototypical examples of physical systems where exotic and fascinating spin phases can be realized [1–4]. Owing to the astonishing manipulation currently achievable in the laboratory, among the variety of spin systems in nature, the spinor Bose-Einstein condensates (BEC) of atomic cold gases confined through optical trapping conforms an ideal platform to investigate such spin phases [5–8]. The first spinor BEC was realized experimentally in 1998 with ^{23}Na atoms of $f = 1$ [9], since then spinorial BECs have already been realized for spins $f = 2, 3, 4, 6$, and 8 [5,10–14].

The spin phases of a BEC can vary not only with respect to the atomic species of the condensate, but also with applied external fields and temperature [4,6,15,16]. At temperatures close to absolute zero, the atomic gas is very well described by a single macroscopic quantum state, a description that remains valid even in the presence of external fields. However, as the temperature is increased, the cloud of thermally excited atoms induces nontrivial spin-spin interactions [15,17,18], leading to the appearance of a number of interesting phenomena, ranging from the appearance of magnetic spin domains, shifts in the phase boundaries, the rise of metastable phases, and to quantum quench dynamics, just to mention a few [8,18–23]. Theoretically, one of the simplest methods to study many-body systems at finite temperatures, such as the BECs, is the Hartree-Fock (HF) approximation [17,24]. The HF approach starts by assuming that the whole condensate at finite temperature can be partitioned in two parts described by a condensate fraction and a thermal cloud of noncondensate atoms. Both fractions are then determined via coupled Gross-Pitaevskii (GP) and HF equations, which are usually solved numerically in a self-consistent manner [15]. However, the analytical derivations and numerical computations for the noncondensate fraction become quickly challenging as one increases the spin-f value, since its degrees of freedom increase as $(2f + 1)^2$. An alternative way to overcome this problem is to take advantage of the following two results: (i) most spin phases of BEC predicted by mean-field theory have symmetries in common with the Hamiltonian [4,25–27], and (ii) the HF theory keeps the symmetries *self-consistent* [24], i.e., the noncondensate fraction inherits the symmetries in common of the condensate fraction and the Hamiltonian. Hence, as we show *a posteriori*, we are able to reduce significantly the degrees of freedom describing the condensate, allowing us, in turn, to gain further insight into its physical properties, such as the magnetization and the atom populations at finite temperatures. In addition, it allows us to inspect the admissible regions of the spin phases that lead to metastable phases and quench dynamics [18,22,28].

In this work we implement a method based in the Majorana representation [29] to determine and fully characterize the noncondensate fraction of atoms for a general spinor BEC having a given point-group symmetry. We draw our attention to families of spin phases of wide interest by the appearance of Abelian and non-Abelian topological excitations [3,4,30,31]. In particular, we study the spin phases that include the

*ed.ensastiga@uliege.be
†fmireles@ens.cnyn.unam.mx

ferromagnetic, polar, and nematic phases, as well as the more exotic phases that are closely related to the platonic solids: tetrahedron, octahedron, cube, and icosahedron.

The paper is organized as follows: In Sec. II we review the Hamiltonian model used for a general spinor BEC, as well as the mean-field and the Hartree-Fock approximations employed to describe the system at zero and finite temperatures. The Majorana representation of pure states is also introduced and applied to describe the ground spin phases of a spin-2 BEC, as well as its phase diagram. The characterization of several noncondensate fractions of spinor BECs, and the physical implications on their multipolar magnetic moments, are explained in Sec. III. Here we describe and make use of the generalization of the Majorana representation for mixed states. In Sec. IV we consider the HF equations at finite temperatures for the spin-2 BEC case, where we focus in the study of the admissible region of each spin phase. We end the paper with some final comments and conclusions in Sec. V.

II. THEORY

A. Spinor BEC Hamiltonian

We consider a BEC of an atomic gas with total spin f confined through an optical trap. The condensate is assumed to be weakly interacting and sufficiently diluted such that only two-body collisions by contact interaction are predominant and the s-wave approximation is still valid. The spinor-quantum field associated to the spinor condensate is denoted by $\hat{\boldsymbol{\Psi}} = (\hat{\psi}_f, \hat{\psi}_{f-1}, \ldots, \hat{\psi}_{-f})^{\mathrm{T}}$, where $\hat{\psi}_m = \hat{\psi}_m(\boldsymbol{r})$ are the field operators for a magnetic quantum number m, and T denotes the transpose. The particle-particle (p-p) interaction terms of the Hamiltonian should be given, in general, by a product of field operators in different positions $V_{p-p}(\boldsymbol{r_1}, \boldsymbol{r_2})\psi_i^\dagger(\boldsymbol{r}_1)\psi_j^\dagger(\boldsymbol{r}_2)\psi_k(\boldsymbol{r}_1)\psi_l(\boldsymbol{r}_2)$. However, since we are considering only point-contact interactions $V_{p-p}(\boldsymbol{r_1}, \boldsymbol{r_2}) \propto \delta(\boldsymbol{r}_1 - \boldsymbol{r}_2)$, the double integration carried over the $\boldsymbol{r}_1$ and $\boldsymbol{r}_2$ spatial variables is then reduced to just one [4,15]. Hence, the full Hamiltonian in the second-quantization formalism reduces to [3,4]

$$\hat{H} = \hat{H}_s + \hat{V} = \int \mathrm{d}\boldsymbol{r} \left\{ \sum_{i,j} [\hat{\psi}_i^\dagger (h_s)_{ij} \hat{\psi}_j] + \hat{v} \right\}, \tag{1}$$

where h_s is the spatial contribution

$$h_s = \left(-\frac{\hbar^2 \nabla^2}{2M} + U(\boldsymbol{r}) \right) \mathbb{1}_{2f+1}, \tag{2}$$

with M the atomic mass, $U(\boldsymbol{r})$ is the potential energy associated to the optical trap, and $\mathbb{1}_{2f+1}$ is the $(2f+1) \times (2f+1)$ unit matrix. The interparticle interactions, included in $\hat{v}$, are also described in the second-quantization formalism and are usually written in terms of the interaction channels with coupling factors c_γ having $\gamma = 0, 1, \ldots f$ [3,4]. Explicitly, the interaction terms are comprised by

$$\hat{v} = \sum_{\gamma=0}^{f} \frac{c_\gamma}{2} \mathcal{M}^{(\gamma)}_{ijkl} \hat{\psi}_i^\dagger \hat{\psi}_j^\dagger \hat{\psi}_k \hat{\psi}_l, \tag{3}$$

where $\mathcal{M}^{(\gamma)}$ are numerical complex tensors independent of the atomic specie. For instance, in the case of spin-2 BEC, there exists only three types of interacting terms [4]:

$$\begin{aligned}
\hat{v} &= \frac{c_0}{2} : \hat{n}^2 : + \frac{c_1}{2} : \hat{\boldsymbol{F}}^2 : + \frac{c_2}{2} \hat{A}_{00}^\dagger \hat{A}_{00}, \\
&= \frac{c_0}{2} : \left(\sum_i \hat{\psi}_i^\dagger \hat{\psi}_i \right)^2 : + \frac{c_1}{2} : \left(\sum_{\alpha,i,j} (F_\alpha)_{ij} \hat{\psi}_i^\dagger \hat{\psi}_j \right)^2 : \\
&\quad + \frac{c_2}{10} \left(\sum_i (-1)^i \hat{\psi}_i^\dagger \hat{\psi}_{-i}^\dagger \right) \left(\sum_i (-1)^i \hat{\psi}_i \hat{\psi}_{-i} \right) \\
&= \frac{c_0}{2} \sum_{i,j} \hat{\psi}_i^\dagger \hat{\psi}_j^\dagger \hat{\psi}_j \hat{\psi}_i + \frac{c_1}{2} \sum_{\alpha,i,j,k,l} (F_\alpha)_{ij} (F_\alpha)_{kl} \hat{\psi}_i^\dagger \hat{\psi}_k^\dagger \hat{\psi}_l \hat{\psi}_j \\
&\quad + \frac{c_2}{10} \left(\sum_i (-1)^i \hat{\psi}_i^\dagger \hat{\psi}_{-i}^\dagger \right) \left(\sum_i (-1)^i \hat{\psi}_i \hat{\psi}_{-i} \right),
\end{aligned} \tag{4}$$

where : : denotes the normal ordering of the field operators and F_α the angular momentum matrices components of spin $f = 2$ along the $\alpha = x, y$ or z axes, written in units of $\hbar$. Hence the entries of the tensors $\mathcal{M}^{(\gamma)}$ are

$$\begin{aligned}
\mathcal{M}^{(0)}_{ijkl} &= \delta_{il}\delta_{jk}, \quad \mathcal{M}^{(1)}_{ijkl} = (F_\alpha)_{il}(F_\alpha)_{jk}, \\
\mathcal{M}^{(2)}_{ijkl} &= \frac{(-1)^{i+k}}{5} \delta_{i,-j}\delta_{k,-l}.
\end{aligned} \tag{5}$$

On the other hand, the coefficients c_γ in (4) are linear combinations of the s-wave scattering lengths of the total spin-F channel a_F ($F = 0, 2, 4$), whose values will depend on the atomic species of the condensate [3,4]. In particular, the c_γ coefficients for the spin-2 BEC case are given by [4]

$$c_0 = \frac{4g_2 + 3g_4}{7}, \quad c_1 = \frac{g_4 - g_2}{7}, \quad c_2 = \frac{7g_0 - 10g_2 + 3g_4}{7}, \tag{6}$$

with

$$g_F = \frac{4\pi\hbar^2}{M} a_F. \tag{7}$$

We plot in Table I the a_F values for spin-2 condensates of ^{23}Na and two isotopes of Rb. The term associated to c_0 is usually called spin-independent interaction, since it is equivalent to the square of the number operator. Clearly, the rest of the interactions are spin dependent. The Hamiltonian (3) has a symmetry group isomorphic to SO(3) $\times \mathbb{Z}_2$ constituted by the group of rotations and the time-reversal symmetry.

B. Mean-field theory

In mean-field (MF) theory one considers that all the atoms in the spinor condensate are in the same quantum state described by a spinor order parameter $\langle \hat{\boldsymbol{\Psi}} \rangle = \boldsymbol{\Phi}$ [3,4]. We assume for simplicity that the spatial and spinorial sectors of the system are factorizable and, consequently, they are mutually independent. Additionally, we consider the box potential with size L [3,33,34], $U(\boldsymbol{r}) = 0$, where the ground state is $\phi_j(\boldsymbol{r}) = \phi_j e^{i\boldsymbol{k}\cdot\boldsymbol{r}}$ with $\boldsymbol{k} = \boldsymbol{0}$ and the spinor order parameter $\boldsymbol{\Phi} = (\phi_f, \phi_{f-1}, \ldots, \phi_{-f})^{\mathrm{T}}$. We consider that L tends to infinity, such that the index $\boldsymbol{k}$ has a three-dimensional domain $\boldsymbol{k} \in \mathbb{R}^3$. We will use this result in Sec. IV. As an illustration

TABLE I. Scattering lengths a_F, extracted from [32], and ratios of the coupling factors c_γ (6) of the atomic species ^{23}Na and two isotopes of Rb.

Atom	M(u)	Scattering length (a_B)			Spin-dependent coupling factors	
		a_4	a_2	a_0	c_1/c_0	c_2/c_0
^{23}Na	22.99	64.5 ± 1.3	45.8 ± 1.1	34.9 ± 1.0	0.05 ± 0.005	-0.05 ± 0.04
^{87}Rb	86.91	106.0 ± 4.0	94.5 ± 3.0	89.4 ± 3.0	0.017 ± 0.007	-0.002 ± 0.06[a]
^{83}Rb	82.92	81.0 ± 3	82.0 ± 3	83.0 ± 3	-0.002 ± 0.007	0.0070 ± 0.07[a]

[a]Here, we decided to leave an extra decimal beyond to the uncertainty scale.

of the MF approximation, let us calculate the MF energy of the spin-2 BEC. The application of MF theory in Eq. (4) leads to the energy of the system,

$$E[\mathbf{\Phi}] = \frac{c_0}{2}(\mathbf{\Phi}^\dagger\mathbf{\Phi})^2 + \frac{c_1}{2}\sum_\alpha(\mathbf{\Phi}^\dagger F_\alpha\mathbf{\Phi})^2 + \frac{c_2}{10}|\mathbf{\Phi}^\dagger\mathcal{T}\mathbf{\Phi}|^2 - \mu(\mathbf{\Phi}^\dagger\mathbf{\Phi} - N), \tag{8}$$

where we constrained the system to a fixed number of particles N, with the Lagrange multiplier being the chemical potential μ. The time-reversal operator $\mathcal{T}$ transforms the spinor $\mathbf{\Phi}$ as

$$\mathcal{T}\Phi_k = (-1)^{f+k}\Phi^*_{-k}. \tag{9}$$

For the following sections, we find it convenient to write the expression (8) in terms of the density matrix of the condensate gas in the MF solution, $\rho = \mathbf{\Phi}\mathbf{\Phi}^\dagger$, where $\mathrm{Tr}\,\rho = N$. Hence,

$$E[\mathbf{\Phi}] = \frac{c_0}{2}\mathrm{Tr}[\rho]^2 + \frac{c_1}{2}\sum_\alpha \mathrm{Tr}[\rho F_\alpha]^2 + \frac{c_2}{10}\mathrm{Tr}[\mathcal{T}\rho\mathcal{T}\rho] - \mu(\mathrm{Tr}[\rho] - N). \tag{10}$$

Note that the spin-independent interaction $\mathrm{Tr}[\rho]^2$ contributes just as a constant term. On the other hand, the other two interactions are spin dependent and, consequently, able to modify the ground state of the system.

C. Symmetries and Majorana representation for pure spin states

The condensate is thus constrained to a fixed density of particles $N = \mathbf{\Phi}^\dagger\mathbf{\Phi}$, where the ground state $\mathbf{\Phi}$ of the BEC minimizes the functional MF energy $E[\mathbf{\Phi}] = \langle\hat{H}\rangle$. It is known that the majority of the ground states of the BEC, without external fields, have rotational symmetries [4,25–27,35]. This result was predicted by Michel's theorem [36], which dictates that, for a real function $\mathcal{F}$ with domain D, $\mathcal{F} : D \to \mathbb{R}$, the points $p \in D$ with symmetries in common with $\mathcal{F}$ may be critical. Consequently, one can find ground states of any spinor BEC by making use of the symmetry subgroups of rotations, as proposed in Ref. [27]. The symmetry point group of a given order parameter $\mathbf{\Phi}$ can be found through the Majorana representation for pure states [29], which is defined via a polynomial that involves the coefficients of $\mathbf{\Phi}$, that reads explicitly

$$p_\psi(Z) = \sum_{m=-f}^{f}(-1)^{f-m}\sqrt{\binom{2f}{f-m}}\phi_m z^{f+m}. \tag{11}$$

The polynomial $p_\psi(z)$ has degree at most $2f$, and by rule, its set of roots $\{\zeta_k\}_k$ is always increased to $2f$ by adding the sufficient number of roots at infinity. Now, we associate to each root $\zeta = \tan(\theta/2)e^{i\phi}$, via the stereographic projection from the south pole, a point on the sphere S^2 with spherical angles (θ, ϕ). Hence, the *constellation* $\mathcal{C}_\psi$ of $|\psi\rangle$ is thus defined as the set of $2f$ points on S^2, called *stars*. When $\mathbf{\Phi}$ is transformed in the Hilbert space by the unitary representation $D(\mathsf{R})$ of a rotation $\mathsf{R} \in \mathrm{SO}(3)$, the constellation rotates by R on the physical space $\mathbb{R}^3$. In addition, the time-reversal operator transforms the Majorana constellation of the spinor $\mathbf{\Phi}$ to the antipodal counterpart [37]. Therefore the quantum state $\mathbf{\Phi}$ shares the same point-group symmetry of the polyhedron associated to the constellation $\mathcal{C}_\mathbf{\Phi}$. More details about the Majorana representation and their applications are found in Refs. [37,38].

D. Spin-phase diagram of spin-2 BEC

To get familiar with the Majorana representation for pure states, we now describe the spin-2 phases with higher point groups. We then produce the phase diagram of the spin-2 BEC in the parameter space (c_1, c_2) (see Fig. 1) by using the symmetry and magnetization properties of the phases. We shall now describe four different ground states:

(1) Ferromagnetic (FM) phase: The spinor order parameter has only one nonzero coefficient, $\phi_2 = \sqrt{N}$. It is symmetric under rotations about the z axis, with the point group isomorphic to the special orthogonal group SO(2). Its constellation $\mathcal{C}_\mathbf{\Phi}$ consists of four coincident points on the north pole. Each atom is fully magnetized along the z axis,

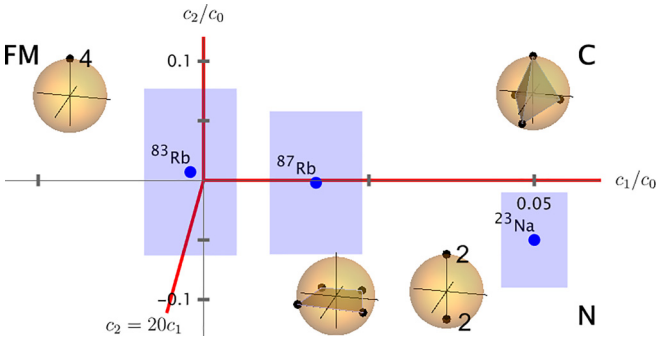

FIG. 1. Diagram phase for spin-2 BECs obtained with MF theory. The Majorana representation of some states of each phase are shown. The adjacent number in some points correspond to its degeneracy. The $(c_1/c_0, c_2/c_0)$ values and their respective uncertainties of the atomic species of spin 2 (see Table I) are marked on the figure.

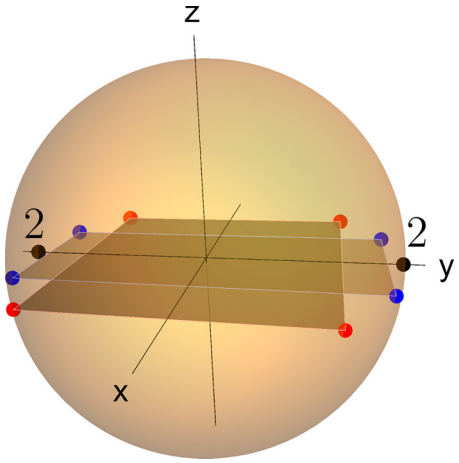

FIG. 2. Majorana constellations of the nematic states of spin-2 BEC with $\eta = \pi/3, 3\pi/8, \pi/2$, shown in color black, blue, and red, respectively.

$M_z \equiv \langle F_z \rangle / N = 2$ and $M_x = M_y = 0$. Hence, the FM phase maximizes the c_1 interaction term $\langle \boldsymbol{F} \rangle^2 = 4N$, whereas its c_2 interaction vanishes $|\langle \mathcal{T} \rangle|^2 = 0$. The FM phase appears for any spin-f condensate and corresponds to the $|f, f\rangle$ phase of the $|f, m\rangle$ family mentioned below.

(2) Nematic family: It consists of a family of quantum states $\boldsymbol{\Phi} = \sqrt{N}(\sin\eta/\sqrt{2}, 0, \cos\eta, 0, \sin\eta/\sqrt{2})^{\mathrm{T}}$ parametrized by $\eta \in [\pi/3, \pi/2]$ [25] (see Fig. 2). Contrary to the FM phase, this state minimizes the c_1 interaction, while maximizing the c_2 interaction, $\langle \boldsymbol{F} \rangle^2 = 0$ and $|\langle \mathcal{T} \rangle|^2 = N$, respectively. There are two exceptional phases of the nematic family:

(2a) Polar (P) phase: Here $\eta = \pi/2$, yielding that $\phi_0 = \sqrt{N}$, and the other terms are equal to zero. Its symmetry group, denoted by D_∞, consists of the group generated by any rotation about the z axis and a rotation by π about any axis on the equator. The constellation of the P phase has two points on each pole of the sphere. This phase exists for any spin-f BEC, being the state $m = 0$ of the $|f, m\rangle$ phases (see Sec. III B).

(2b) Square (S) phase: It is obtained when $\eta = 0$, and its nonzero order-parameter terms are $\phi_2 = \phi_{-2} = \sqrt{N/2}$. Its Majorana constellation consists of a square. Hence, $\boldsymbol{\Phi}$ has the dihedral point group denoted by D_4 [39]. This phase belongs to the class of NOON spin states that we describe in Sec. III B.

(3) Tetrahedron (T) phase: This spin-2 phase has $\boldsymbol{\Phi} = \sqrt{N/3}(1, 0, 0, \sqrt{2}, 0)^{\mathrm{T}}$. The order parameter has a constellation forming a tetrahedron. Hence, its symmetry group is the tetrahedron point group denoted by T in the Schönflies notation [39]. It has null magnetization, and it is orthogonal to its antipodal state, yielding both spin-dependent interactions equal to zero, $\langle \boldsymbol{F} \rangle^2 = |\langle \mathcal{T} \rangle|^2 = 0$. This phase is also called the cyclic phase C [32,40].

We remark that a generic nematic phase is a quantum superposition of the polar and square phases. An analogous degenerate family was found earlier by Mermin in the context of d-wave pairing [41]. The phases mentioned above also appear when we consider other terms in the Hamiltonian, such as linear and quadratic Zeeman terms [4,32]. We plot in Fig. 1 the Majorana constellation associated to each phase discussed above, including the square and polar constellations of the nematic family. Given the symmetry and magnetization properties mentioned above, we can now deduce the ground spin phases by analyzing each quadrant of the (c_1, c_2) parameter space:

(1) Quadrant $c_1 > 0$ and $c_2 > 0$: The ground state is given by the solution that minimizes both interactions. In this region the spinor order parameter is the cyclic phase.

(2) Quadrant $c_1 > 0$ and $c_2 < 0$: The ground state is such that minimizes $\langle \boldsymbol{F} \rangle^2$ and maximizes $|\langle \mathcal{T} \rangle|^2$. The state that fulfills these conditions is the N phase.

(3) Quadrant $c_1 < 0$ and $c_2 > 0$: In this case we have the opposite conditions from the ones mentioned in (2), which are fulfilled by the FM phase.

(4) Quadrant $c_1 < 0$ and $c_2 < 0$: Here we need to compare between the minimal values attained by both interaction terms, taking into account that $|\boldsymbol{\Phi}|^2 = N$. The minimums of the c_1 and c_2 terms are $2c_1N^2$ and $c_2N^2/10$, respectively. Hence, the ground state is the FM phase when $20c_1 \leqslant c_2$ and the N phase otherwise.

We plot in Fig. 1 the ground-state spin-phase diagram of spin-2 BEC. All the phase transitions are of first order, since at least one of the order-parameter coefficients changes drastically over each phase boundary.

E. Hartree-Fock approximation

In BECs, the simplest many-body theory that goes beyond MF theory, and is capable of capturing the relevant physics occurring in its spin-phase diagrams, as well as in its concomitant boundary regions, is the Hartree-Fock approximation [15,17,18,24]. HF theory is robust when describing spinor condensates at finite but ultracold temperatures [15,17,42]. Formally, the field operator in the HF approximation is given by the order parameter plus an inhomogeneous variational perturbation, $\hat{\psi}_j(\boldsymbol{r}) = \phi_j(\boldsymbol{r}) + \hat{\delta}_j(\boldsymbol{r})$. The physical picture is that the cold atomic gas is assumed to be formed by two portions: the condensate (c) and the noncondensate (nc) atomic fractions. Each fraction of the atomic gas is then represented by a density matrix $\rho^c_{ij} = \phi_i\phi^*_j$ and $\rho^{nc}_{ij} = \langle \hat{\delta}^\dagger_j \hat{\delta}_i \rangle$, composed of pure and mixed quantum states, respectively. The atomic fraction of each part is given by $N^a = \mathrm{Tr}(\rho^a)$ for $a = n, nc$, and satisfies $N^c + N^{nc} = N$. The noncondensate atoms ρ^{nc} act as a cloud of excited atoms that interacts nontrivially with the condensate fraction ρ^c. The full one-body density matrix that represents the noncondensate fraction is given by $\rho^{nc}_{ij}(\boldsymbol{r}_1, \boldsymbol{r}_2) = \langle \hat{\delta}^\dagger_j(\boldsymbol{r}_1)\hat{\delta}_i(\boldsymbol{r}_2) \rangle$ with off-diagonal terms in the spatial ($\boldsymbol{r}_1 \neq \boldsymbol{r}_2$) and spinorial parts ($i \neq j$). However, since we are only considering point-contact interactions among the atoms, the off-diagonal spatial terms are not relevant for the formulation of the HF equations in the spinorial part [15]. As we observe *a posteriori* in Sec. IV, only the terms $\rho^{nc}_{ij} = \rho^{nc}_{ij}(\boldsymbol{r}, \boldsymbol{r})$ are needed to determine the population fractions in the spin eigenstates. Besides, since we are working in the box confinement potential, the order parameter $\phi_j(\boldsymbol{r})$ turns spatially homogeneous, as we described in Sec. II B. The total system is denoted by $\rho = \rho^c + \rho^{nc}$, with $\mathrm{Tr}\rho = N$. There may exist other contributions in the system due to other correlations, such as the Popov anomalous density $\langle \hat{\delta}_i \hat{\delta}_j \rangle$ and the three-field correlations $\langle \hat{\delta}_i \hat{\delta}_j \hat{\delta}^\dagger_k \rangle$ [43]. However, a reasonable

approximation is to neglect them, which is valid for diluted atomic gases at finite ultracold temperatures below the condensation temperature [18,43]. The maximum temperature, where the HF theory with the previous approximations predicts a spin phase, can be estimated by the condensation temperature $T_c^{\rm spin}$ of an ideal spin-f BEC trapped in a box. It is known that $T_c^{\rm spin}$ is equal to the condensation temperature of an ideal scalar gas T_0 [34] rescaled by the internal spin states $T_c^{\rm spin} = (2f+1)^{-2/3} T_0$ [15], where

$$T_0 = 3.31\hbar^2 N^{2/3}/(k_B M), \tag{12}$$

with k_B the Boltzmann constant. As an example, for BEC with Na^{23} atoms with a typical density achieved in experiments $N = 10^{14}$ cm^{-3} [44], $T_0 = 1.5$ μK, and then $T_c^{\rm spin} \approx 0.72$ μK, 0.51 μK for $f = 1$ and 2, respectively. As we emphasize in the following sections, even in the scenario in which the fraction associated to ρ^{nc} is small compared to that associated to ρ^c, new interactions of the type $\rho^c \leftrightarrow \rho^{nc}$ and $\rho^{nc} \leftrightarrow \rho^{nc}$ emerge owing to the nontrivial collisions among the atoms. Consequently, important modifications of the physical properties of the BEC can take place, such as strength changes of the magnetization, shifting of the phase-transition boundaries, and variations of the allowed region for the metastable phases [15,18]. Operationally, those new extra two-body interaction terms, called direct and exchange interactions, are calculated through the use of the Wick theorem (see, e.g., p. 89 of Ref. [24]):

$$\begin{aligned}\langle \hat\psi_i^\dagger \hat\psi_j^\dagger \hat\psi_k \hat\psi_l\rangle = {}& \rho^c_{ik}\rho^c_{jl} + \rho^{nc}_{ik}\rho^{nc}_{jl} + \rho^{nc}_{il}\rho^{nc}_{jk} \\ & + \rho^c_{ik}\rho^{nc}_{jl} + \rho^c_{il}\rho^{nc}_{jk} + \rho^c_{jk}\rho^{nc}_{il} + \rho^c_{jl}\rho^{nc}_{ik}. \end{aligned} \tag{13}$$

Note that $\rho^c_{ik}\rho^c_{jl} = \rho^c_{jk}\rho^c_{il}$, since the condensate fraction is represented by a pure quantum state. As an example to the previous equation, we express the c_γ spin interactions obtained in the HF theory for $\gamma = 0, 1, 2$ (4), which reads

$$\begin{aligned}\langle \hat\psi_i^\dagger \hat\psi_j^\dagger \hat\psi_j \hat\psi_i\rangle &\approx \{{\rm Tr}[\rho^c + \rho^{nc}]\}^2 + {\rm Tr}[\rho^{nc}(2\rho^c + \rho^{nc})] \\ &= N^2 + {\rm Tr}[\rho^{nc}(2\rho^c + \rho^{nc})], \end{aligned} \tag{14}$$

$$\begin{aligned}&\sum_\alpha (F_\alpha)_{il}(F_\alpha)_{jk}\langle \hat\psi_i^\dagger \hat\psi_j^\dagger \hat\psi_k \hat\psi_l\rangle \\ &\quad\approx \sum_\alpha \{{\rm Tr}[\rho F_\alpha]^2 + {\rm Tr}[F_\alpha \rho^{nc} F_\alpha(2\rho^c + \rho^{nc})]\}, \end{aligned} \tag{15}$$

$$\langle \hat A_{00}^\dagger \hat A_{00}\rangle \approx \frac{1}{2f+1}{\rm Tr}[\mathcal{T}\rho\mathcal{T}\rho + \mathcal{T}\rho^{nc}\mathcal{T}(2\rho^c + \rho^{nc})], \tag{16}$$

where we use the Einstein summation convention for the Latin repeated indices. The time-reversal operator $\mathcal{T}$ acts in ρ as

$$(\mathcal{T}\rho\mathcal{T})_{ji} = (-1)^{2f-i-j}\rho_{-i-j}. \tag{17}$$

III. CHARACTERIZATION OF THE NONCONDENSATE FRACTION

A generic noncondensate fraction of a BEC of spin f has $(2f+1)^2$ degrees of freedom. However, for systems with a self-consistent symmetry, i.e., for cases such that the nonperturbed phase ρ^c and the Hamiltonian of the system $\hat H$ have some symmetries in common, the noncondensate fraction ρ^{nc} inherits such symmetries, and when solving the GP equations of the BEC, its degrees of freedom are reduced significantly (see [24] for further details). This leaves us now to determine the mixed states ρ^{nc} that share the common symmetries with the order parameter $\mathbf{\Phi}$ and the full Hamiltonian (3). To that aim, we make use of a generalization of the Majorana representation for mixed states [45] to exploit the point-group symmetries of the phases. The following results are valid at any temperature. Besides, they are not independent to the analytical dependency of the noncondensate fraction with the temperature. The finite-temperature effects will be discussed in Sec. IV.

A. Majorana representation for mixed states

Let $\mathcal{B}_f$ be the set of the density matrices of spin-f states. Thus $\mathcal{B}_f$ is equivalent to the set of $(2f+1)\times(2f+1)$ complex matrices which satisfy the following properties [37]:

(1) $\rho^\dagger = \rho$, (Hermiticity)
(2) ${\rm Tr}(\rho) = 1$, (Unit trace)
(3) $\rho \geqslant 0$, (Semipositive condition).

Observe that for a BEC, the total ρ, the condensate ρ^c, and the noncondensate ρ^{nc} fractions of the atoms belong to the set of mixed states with the exception that their traces are different, where ${\rm Tr}(\rho^a) = N^a$, where $a = n, nc$, or are omitted for the whole system. In $\mathcal{B}_f$ exists an orthonormal basis given by the set of the tensor operators $T_{\sigma\mu}$ with $\sigma = 0, \ldots 2f$ and $\mu = -\sigma, \ldots, \sigma$ [46–48], which are written in terms of the Clebsch-Gordan coefficients $C^{jm}_{j_1 m_1 j_2 m_2}$ and read

$$T_{\sigma\mu} = \sum_{m,m'=-f}^{f} (-1)^{f-m'} C^{\sigma\mu}_{fm,f-m'} \,|f,m\rangle\,\langle f,m'|\,, \tag{18}$$

satisfying the following properties:

$${\rm Tr}(T^\dagger_{\sigma_1\mu_1} T_{\sigma_2\mu_2}) = \delta_{\sigma_1\sigma_2}\delta_{\mu_1\mu_2}, \quad T^\dagger_{\sigma\mu} = (-1)^\mu T_{\sigma-\mu}. \tag{19}$$

The key property of this basis is that they transform block diagonally under a unitary transformation $U(\mathsf{R})$, that represents a rotation $\mathsf{R} \in {\rm SO}(3)$, according to an *irrep* of ${\rm SO}(3)$ $D^{(\sigma)}(\mathsf{R})$, such that

$$U(\mathsf{R}) T_{\sigma\mu} U^{-1}(\mathsf{R}) = \sum_{\mu'=-\sigma}^{\sigma} D^{(\sigma)}_{\mu'\mu}(\mathsf{R}) T_{\sigma\mu'}, \tag{20}$$

where $D^{(\sigma)}_{\mu'\mu}(\mathsf{R}) \equiv \langle \sigma,\ \mu'|e^{-i\alpha F_z} e^{-i\beta F_y} e^{-i\gamma F_z}|\sigma,\ \mu\rangle$ is the Wigner D matrix [48] of a rotation R with Euler angles $(\alpha,\ \beta,\ \gamma)$, and $\sigma = 0, 1, 2, \ldots$ labels the irrep. The noncondensate fraction ρ^{nc} of a spinor BEC can thus be written in terms of this basis,

$$\rho^{nc} = N^{nc}\left(\frac{\mathbb{1}_f}{2f+1} + \sum_{\sigma=1}^{2f} \boldsymbol{\rho}_\sigma \cdot \boldsymbol{T}_\sigma\right), \tag{21}$$

where $\boldsymbol{\rho}_\sigma = (\rho_{\sigma\sigma}, \ldots, \rho_{\sigma-\sigma}) \in \mathbb{C}^{2\sigma+1}$, with $\rho_{\sigma\mu} = {\rm Tr}(\rho\, T^\dagger_{\sigma\mu})$, $\boldsymbol{T}_\sigma = (T_{\sigma\sigma}, \ldots, T_{\sigma,-\sigma})$ is vector of matrices, and the dot product is the short for $\sum_{\mu=-\sigma}^{\sigma} \rho_{\sigma\mu} T_{\sigma\mu}$. The properties of the density matrices and the tensor operators imply that each $\boldsymbol{\rho}_\sigma$ vector can be associated to a constellation *à la Majorana* (11) consisting of 2σ points on S^2. The hermiticity condition of ρ^{nc} and Eq. (19) impy that the constellation of every $\boldsymbol{\rho}_\sigma$ has antipodal symmetry [45]. As

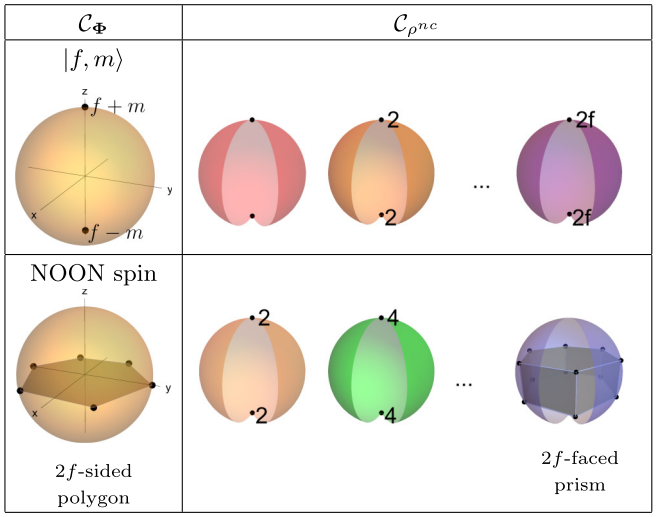

FIG. 3. Majorana representation of mixed states of the families $|f,m\rangle$ and NOON spin states.

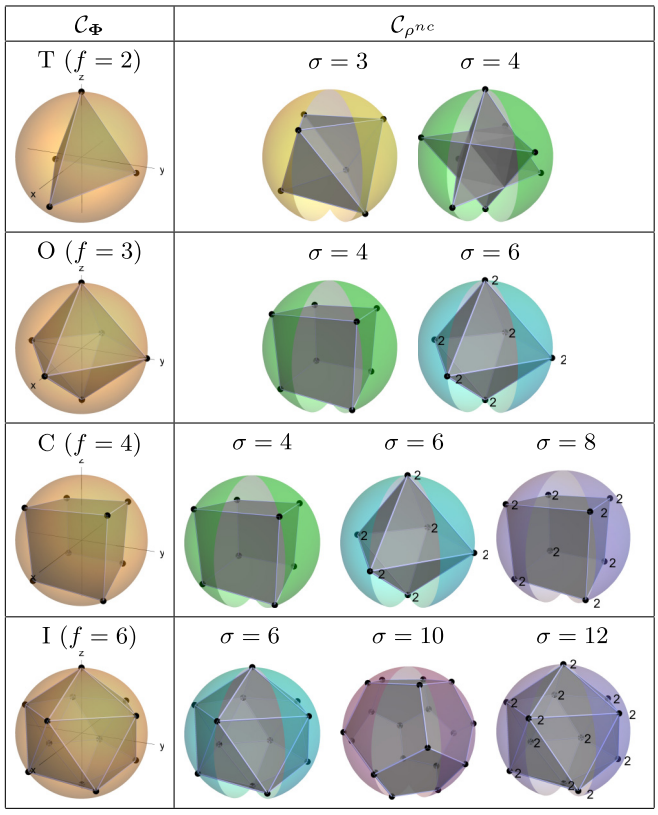

FIG. 4. Majorana representation of mixed states with a point group equal to a platonic solid: tetrahedron (T), octahedron (O), cube (C), and icosahedron (I). The radii of the spheres of $\mathcal{C}_{\rho^{nc}}$ are arbitrary up to the semidefinite condition of ρ^{nc}.

it is explained in Ref. [45], the norm and complex phase factor of each $\boldsymbol{\rho}_\sigma$ are relevant to specify ρ^{nc}. The norm of $\boldsymbol{\rho}_\sigma$, denoted by r_σ, can be associated to the radius of the sphere. On the other hand, by the hermiticity of ρ^{nc}, there are only two options, both differing by a minus sign [45]. We present in Appendix A a method, based on Ref. [45], to associate the phase factor to a certain equivalence class of points in the constellation. For our purposes to determine the noncondensate fraction with a particular point group, it is sufficient to add the choice of sign to the radius r_σ, despite that the sign is not considered to define the radius of the spheres. Therefore a mixed state is associated to a set of $2f$ constellations, denoted by $\mathcal{C}_{\rho^{nc}}$, with antipodal symmetry over spheres with radii r_σ, respectively. In particular, ρ^{nc} has a point group G if and only if all the constellations of the $\boldsymbol{\rho}_\sigma$ vectors share the same symmetry:

$$D^{(\sigma)}(g)\boldsymbol{\rho}_\sigma = \boldsymbol{\rho}_\sigma, \quad \text{for each } g \in G. \tag{22}$$

B. Applications: Spin phases and magnetic moments

Let us now analyze the set of mixed states with a specific point-group symmetries. We study three families of spin phases: (A) $|f,m\rangle$ states, (B) NOON states, and (C) the spin phases associated with a platonic solid. Their respective Majorana constellations of ρ^{nc} are summarized in Figs. 3 and 4. We also calculate its corresponding eigenspectrum for the cases that it is possible to obtain analytical expressions, and that will be helpful in the next section. In addition, we discuss the multipolar magnetic moments of the spin phases which are closely related, as we explain below, to the Majorana representations of each state ρ.

The magnetic moment of kth- order, or $(k+1)$th polar magnetic moment, per atom, can be determined through the rank-k spin nematic tensors $N_{\nu_1\nu_2\ldots\nu_k}$ as follows [4]:

$$M_{\nu_1\nu_2\ldots\nu_k} \equiv \frac{\mathrm{Tr}(\rho^a N_{\nu_1\nu_2\ldots\nu_k})}{\mathrm{Tr}\rho^a}, \tag{23}$$

with $a=n,\ nc$ (or omitted for the total system), and where

$$N_{\nu_1\nu_2\ldots\nu_k} \equiv \frac{1}{k!}\sum_{\pi\in P_k} F_{\pi(\nu_1)}F_{\pi(\nu_2)}\ldots F_{\pi(\nu_k)}. \tag{24}$$

Here π represents the elements of the permutation group of k objects P_k. For instance, the dipolar and quadrupolar magnetic moments are simply defined by the operators

$$N_\nu = F_\nu, \quad N_{\nu_1\nu_2} = \frac{F_{\nu_1}F_{\nu_2}+F_{\nu_2}F_{\nu_1}}{2}. \tag{25}$$

Recall that the angular momentum operators F_ν are proportional to the tensor operators $T_{1\mu}$ [48],

$$F_z = wT_{10}, \quad F_\pm = \mp\sqrt{2}wT_{1,\pm1}, \tag{26}$$

with $w=\sqrt{f(f+1)(2f+1)/3}$ and $F_\pm = F_x \pm iF_y$. By addition of the angular momentum operator, and for $k \leqslant 2f$, the magnetic moment of kth order is a linear combination of the tensor operators $T_{\sigma\mu}$ with order at most $\sigma \leqslant k$ and $|\mu| \leqslant \Delta$,

$$N_{\nu_1\nu_2\ldots\nu_k} = \sum_{\sigma=0}^{k}\sum_{\mu=-\Delta}^{\Delta} b_{\sigma\mu}T_{\sigma\mu}, \tag{27}$$

where Δ is equal to the total number of x and y subindexes of $N_{\nu_1\ldots\nu_k}$, and $b_{\sigma\mu}$ are complex numbers. The explicit decomposition can be obtained by using recursively the formula of the

product of two tensor operators [48]

$$T_{l_1 m_1} T_{l_2 m_2} = \sum_{l,m} \chi(l_1, l_2, l; f) C^{lm}_{l_1 m_1, l_2 m_2} T_{lm}, \tag{28}$$

with

$$\chi(l_1, l_2, l; f) \equiv (-1)^{2l_2 + l - 2f} \sqrt{(2l_1 + 1)(2l_2 + 1)} \times \begin{Bmatrix} l_1 & l_2 & l \\ f & f & f \end{Bmatrix} \tag{29}$$

written in terms of the $6j$ symbol [48]. As an example, we calculate the terms of the second magnetic moment $N_{\nu_1 \nu_2}$ in Appendix B.

The previous results restrict the possible magnetic moments of a condensate ρ with rotational symmetries because, as we will show later, they have several vectors such as $\boldsymbol{\rho}_\sigma = 0$ for $\sigma \leqslant k$. Consequently, some phases of spinor BEC will have isotropic magnetic moments with respect to the physical space, i.e., $M_{\nu_1 \ldots \nu_k} \propto N^{nc} \mathbb{1}_{\nu_1 \ldots \nu_k}$, where $\mathbb{1}_{\nu_1 \ldots \nu_k}$ are the components of the identity tensor of k indices. The results are also extended to the different fractions n and nc, as well as the total system, because all their respective density matrices are represented in the general expression of ρ^{nc} with a given point-group symmetry.

In the following we will describe the isotropic kth magnetic moments for the spin-phase families of interest. It is also important to remark that states with vanishing expectation values of the tensor operators $T_{\sigma\mu}$ are of great relevance in quantum information and quantum metrology, for instance, a property called anticoherence [49,50], which in turn is connected to multipartite entanglement [51,52] and the susceptibility to detect rotations of quantum systems [53–55]. A useful result that we are going to use later is that the anticoherence order of a spin state is equal to its maximal order of homogeneous kth magnetic moment [50], since, by definition, a spin state ρ is anticoherent of order k if its $\rho_{\sigma\mu}$ components are zero for any $0 < \sigma \leqslant t$ and $|\mu| \leqslant \sigma$.

1. $|f, m\rangle$ phases

The simplest family we address in this work is the set of F_z eigenvectors $|f, m\rangle$, with spinor order parameter $\phi_k \propto \delta_{km}$. The family contains all the states with a continuous point group SO(2), equivalent to rotations about the z axis. The case $m = 0$ has the time-reversal operator as an additional symmetry. Thus the corresponding ρ^{nc} of this family would be diagonal over the $\{|f, m\rangle\}$ basis:

$$\rho^{nc} = \sum_{m=-f}^{f} \lambda_m |f, m\rangle \langle f, m| . \tag{30}$$

In terms of the Majorana representation of mixed states, the components of the $\boldsymbol{\rho}_\sigma$ vectors are

$$\rho_{\sigma\mu} = r_\sigma \delta_{\mu 0}, \tag{31}$$

where the norms of the vectors are linear combinations of the eigenvalues λ_m. The constellations of $\mathcal{C}_{\rho^{nc}}$ have σ points on each pole (see Fig. 3). The additional symmetry associated to the $|f, 0\rangle$ spin phase yields that $\lambda_m = \lambda_{-m}$; consequently, the $\boldsymbol{\rho}_\sigma$ for σ odd are zero. Some examples of the $|f, m\rangle$ phases are the FM and P phases of a spin-2 BEC, which are proportional to the $|2, 2\rangle$ and $|2, 0\rangle$ spin states, respectively.

The eigenspectrum (30) of ρ^{nc} implies that the only nonvanishing terms in $M_{\nu_1 \ldots \nu_k}$ are given by $T_{\sigma 0}$ terms. For instance, the first two magnetic moments are given by

$$M_\nu = \delta_{\nu z} \sum_{m=-f}^{f} m \Lambda_m = \delta_{\nu z} w N^{nc} \rho_{10}, \tag{32}$$

and

$$\begin{aligned} M_{xy} &= M_{xz} = M_{yz} = 0, \\ M_{zz} &= \frac{f(f+1) N^{nc}}{3} + \frac{1}{6\sqrt{5}} \sqrt{\frac{(2f+3)!}{(2f-2)!}} \rho_{20}, \\ M_{xx} &= M_{yy} = \frac{f(f+1) N^{nc}}{3} - \frac{1}{12\sqrt{5}} \sqrt{\frac{(2f+3)!}{(2f-2)!}} \rho_{20}, \end{aligned} \tag{33}$$

where we use the equations deduced in Appendix B, and the fact that $T_{00} = \mathbb{1}/\sqrt{2f+1}$. In particular, let us notice that the $|f, 0\rangle$ spin phase, equivalent to the polar phase, must have $M_\nu = 0$.

2. NOON spin phases

The family consists of the spin phases $\boldsymbol{\Phi}$ with components of the form

$$\phi_m \propto (\delta_{f,m} + \delta_{-f,m})/\sqrt{2}, \tag{34}$$

that we define as the NOON spin phases, since they are the equivalent of a quantum superposition of $2f$ spin-1/2 states pointing about orthogonal directions [56]. The square (S) spin-2 phase is an example of the NOON spin phase. Its point group is equal to D_{2f} in the Schönflies notation [39], which is equivalent to the point group associated to the regular $2f$-agon. The coefficients of $\boldsymbol{\rho}_\sigma$ of the noncondensate fraction are

$$\rho_{\sigma\mu} = \begin{cases} r_\sigma \delta_{\mu 0} & \text{if } \sigma < 2f, \sigma \text{ even} \\ r_{2f} \left(\sin x \, \delta_{\mu 0} + \frac{\cos x}{\sqrt{2}} \delta_{\mu, \pm 2f} \right) & \text{if } \sigma = 2f \\ 0 & \text{otherwise} \end{cases} . \tag{35}$$

Thus the constellations are conformed by all the σ points in each pole for $\sigma < 2f$, and by a regular n-agon prism for $\sigma = 2f$, where its height is dependent on the variable x. Consequently, the $\boldsymbol{\rho}_\sigma$ vectors of the NOON and $|f, 0\rangle$ spin phases are equal except for $\sigma = 2f$ [see Eqs. (31)–(35)]. This implies that the kth magnetic moments $M_{\nu_1 \ldots \nu_k}$ [Eq. (27)] of ρ^{nc} of the NOON and $|f, 0\rangle$ spin phases have the same expressions for $k < 2f$. Therefore, assuming that just the magnetization of the condensate is being measured, the NOON and the $|f, 0\rangle$ spin phases can only be distinguished by its $(2f)$th magnetic moment. Favorably, the eigenspectrum $(\lambda_\nu, \boldsymbol{v}_\nu)$ of the NOON phase can be diagonalized analytically for a general spin value f. It includes $(f-1)$ pairs of degenerate eigenvectors, $\boldsymbol{v}_{2k-1}$ and $\boldsymbol{v}_{2k}$, with $\lambda_{2k-1} = \lambda_{2k}$ and where k goes from 1 to $(f-1)$. The components of the eigenvectors $v_{\nu,m}$ are given by

$$\begin{aligned} v_{1,m} &= \delta_{m,f-1}, \quad v_{2,m} = \delta_{m,-f+1}, \\ v_{3,m} &= \delta_{m,f-2}, \quad v_{4,m} = \delta_{m,-f+2}, \end{aligned}$$

$$\vdots \qquad \vdots$$
$$v_{2f-3,m} = \delta_{m,1}, \quad v_{2f-2,m} = \delta_{m,-1}. \tag{36}$$

There are also three eigenvectors not necessarily degenerate,

$$v_{2f-1,m} = \delta_{m0}, \quad v_{2f,m} = \frac{1}{\sqrt{2}}(\delta_{m,-f} - \delta_{m,f}),$$
$$v_{2f+1,m} = \frac{1}{\sqrt{2}}(\delta_{m,-f} + \delta_{m,f}), \tag{37}$$

where the last eigenvector is proportional to the order parameter $\mathbf{\Phi}$ (34).

3. Platonic phases

Spin phases of BEC with point-group symmetry corresponding to that of the platonic solids—tetrahedron (T), octahedron (O), cube (C), and icosahedron (I)—appear for condensates with spin $f = 2, 3, 4$, and 6, respectively [15,27]. Here, we shall not characterize the spin phase of ρ^{nc} having the point-group symmetry of the dodecahedron, corresponding to a BEC spin phase with $f = 10$. In any case, it is noteworthy that a spin-10 BEC has yet to be developed in laboratory. We now proceed to enlist the properties of each platonic phase of interest, along with its corresponding nonzero components of the $\rho_{\sigma\mu}$ vectors:

(1) Tetrahedron (T) phase:

$$\rho_{3\mp3} = \pm\frac{\sqrt{2}}{3}, \quad \rho_{4\mp3} = \pm\sqrt{\frac{10}{27}},$$
$$\rho_{30} = \frac{\sqrt{5}}{3}, \quad \rho_{40} = -\sqrt{\frac{7}{27}}. \tag{38}$$

The constellations $\mathcal{C}_{\rho^{nc}}$ form an octahedron and a pair of antipodal tetrahedrons, respectively. It is easy to demonstrate that such constellations have the symmetry T, since the point group T belongs to the point group of the octahedron O. Due to the vanishing $\boldsymbol{\rho}_\sigma$ vectors of $\sigma = 1, 2$ for the T phase, the first two magnetic moments are isotropic, implying that

$$M_\nu = 0, \quad M_{\nu_1\nu_2} = 2\delta_{\nu_1\nu_2}N^{nc}. \tag{39}$$

For a lower spin $f = 1$, a phase with this magnetization is forbidden. Hence, it can be said that the T phase is the first spin phase with its first two multipolar magnetic moments isotropic. To obtain isotropic magnetic moments of higher order, one must consider a spin BEC of higher spin.

Let us now show that the noncondensate fraction ρ^{nc} of the T phase has only three degrees of freedom (N^{nc}, r_3, r_4). This reduction allows us to easily calculate the eigenspectrum of ρ^{nc} analytically, since its characteristic polynomial, of degree 5, leads to two nondegenerate roots and a set of threefold degenerate roots. The exact eigenspectrum is given by

$$\Lambda_1 = \Lambda_2 = \Lambda_5 = \frac{1}{5} - \sqrt{\frac{2}{15}}r_4,$$
$$\Lambda_{3,4} = \frac{1}{10}(2 \mp 5\sqrt{2}r_3 + \sqrt{30}r_4),$$
$$\boldsymbol{v}_1 = (0, 0, 1, 0, 0)^{\mathrm{T}},$$
$$\boldsymbol{v}_2 = (0, 1, 0, 0, \sqrt{2})^{\mathrm{T}}/\sqrt{3},$$
$$\boldsymbol{v}_3 = (0, -\sqrt{2}, 0, 0, 1)^{\mathrm{T}}/\sqrt{3},$$
$$\boldsymbol{v}_4 = (1, 0, 0, \sqrt{2}, 0)^{\mathrm{T}}/\sqrt{3},$$
$$\boldsymbol{v}_5 = (-\sqrt{2}, 0, 0, 1, 0)^{\mathrm{T}}/\sqrt{3}. \tag{40}$$

The density matrix ρ^{nc} is a physical state (with nonnegative eigenvalues) if the variables (r_3, r_4) fulfill the condition $5|r_3| \leqslant \sqrt{2} + \sqrt{15}r_4$, with $r_3 \in [-\frac{1}{\sqrt{2}}, \frac{1}{\sqrt{2}}]$ and $r_4 \in [-\sqrt{\frac{2}{15}}\sqrt{\frac{3}{10}}]$.

(2) Octahedron (O) phase:

$$\rho_{4\pm4} = \sqrt{\frac{5}{24}}, \quad \rho_{6\pm4} = -\sqrt{\frac{7}{16}},$$
$$\rho_{40} = \sqrt{\frac{7}{12}}, \quad \rho_{60} = \frac{1}{\sqrt{8}}, \tag{41}$$

with constellations describing a cube for $\sigma = 4$, and an octahedron for $\sigma = 6$ with all its stars having degeneracy equal to 2. The cube and the octahedron belong to the same point-group symmetry, the alternate group A_4 [39], as they are dual geometrical figures. The O phase is the first spin phase with its first three magnetic moments isotropic:

$$M_\nu = M_{\nu_1\nu_2\nu_3} = 0, \quad M_{\nu_1\nu_2} = 4N^{nc}\delta_{\nu_1\nu_2}, \tag{42}$$

since $\boldsymbol{\rho}_\sigma = 0$ for $\sigma = 1, 2, 3$. The proof that the nonexistence of a spin phase with the same property for $f \leqslant 2$ comes from the fact that there are no spin-f states with anticoherence of order 2 for $f < 2$ [52].

(3) Cube (C) phase:

$$\rho_{8\pm8} = \sqrt{\frac{65}{384}},$$
$$\rho_{4\pm4} = \sqrt{\frac{5}{24}}, \quad \rho_{6\pm4} = -\frac{\sqrt{7}}{16}, \quad \rho_{8\pm4} = \sqrt{\frac{7}{96}},$$
$$\rho_{40} = \sqrt{\frac{7}{12}}, \quad \rho_{60} = \frac{1}{\sqrt{8}}, \quad \rho_{80} = \frac{\sqrt{33}}{8}. \tag{43}$$

Then $\mathcal{C}_{\rho^{nc}}$ has three constellations conformed by a cube for $\sigma = 4$ and 8, and by an octahedron for $\sigma = 6$. The stars of the constellations of $\sigma = 6$ and 8 are twofold degenerate. Similarly as the O phase, the C phase has isotropic magnetic moments of order $\sigma = 1, 2, 3$.

(4) Icosahedron (I) phase:

$$\rho_{10\pm10} = \sqrt{\frac{187}{1875}}, \quad \rho_{12\pm10} = \sqrt{\frac{741}{3125}},$$
$$\rho_{6\pm5} = \pm\frac{\sqrt{7}}{5}, \quad \rho_{10\pm5} = \pm\frac{\sqrt{209}}{25}, \quad \rho_{12\pm5} = \mp\sqrt{\frac{286}{3125}},$$
$$\rho_{60} = -\frac{\sqrt{11}}{5}, \quad \rho_{100} = \sqrt{\frac{247}{1875}}, \quad \rho_{120} = 3\sqrt{\frac{119}{3125}}. \tag{44}$$

Here, as it is expected, the constellations are conformed by icosahedrons and dodecahedrons, because they are dual polyhedra, with the point group isomorphic to the alternate group A_5. The stars of the constellation of $\sigma = 12$ are doubly degenerated. The Majorana representation of the I phase tells us that the first five multipolar magnetic moments are isotropic.

The I phase is the first spin value with this property, since there are no anticoherent spin states of order 5 for spin values $f < 6$ [57].

IV. FINITE TEMPERATURES

Once we have characterized the possible noncondensate fractions ρ^{nc} with a particular point-group symmetry, we can use them to study a spinor BEC condensate in a model with self-consistent symmetries. In this section we derive within the HF approximation the equations that define the temperature-dependent condensate and noncondensate fractions, ρ^{c} and ρ^{nc}, of a spin-2 BEC. Next, we exploit the results discussed in the previous section that will allow us to reduce significantly the calculations and yields to analytical expressions of some physical quantities of the spin phases. In particular, we determine the eigenenergies of the atoms in the thermal cloud, and the allowed regions of each spin at finite temperatures.

A. HF equations for spin-2 BECs

We start by writing explicitly the HF energy of a spin-2 BEC by using the equations Eqs. (14)–(16) containing all the spin interactions:

$$\begin{aligned} E_{HF} = E_s &+ \frac{c_0}{2}\{N^2 + \mathrm{Tr}[\rho^{nc}(2\rho^{c} + \rho^{nc})]\} \\ &+ \frac{c_1}{2}\sum_{\alpha}\{\mathrm{Tr}[\rho F_\alpha]^2 + \mathrm{Tr}[F_\alpha \rho^{nc} F_\alpha(2\rho^{c} + \rho^{nc})]\} \\ &+ \frac{c_2}{10}\{\mathrm{Tr}[\mathcal{T}\rho\mathcal{T}\rho + \mathcal{T}\rho^{nc}\mathcal{T}(2\rho^{c} + \rho^{nc})]\} \\ &- \mu(\mathrm{Tr}\rho - N). \end{aligned} \tag{45}$$

The new two-body interactions with respect to the MF energy are the direct and exchange interactions, respectively. Here, E_s is the spatial energy associated to h_s in Eq. (3). In our case $U(\boldsymbol{r}) = 0$, the spatial eigenstates are labeled by the wave vector $\boldsymbol{k}$, and their corresponding eigenenergies are $E_s = \hbar^2 k^2/2M$, i.e., just the kinetic energy. The effect of each term over the spin coherence and the distribution of the atoms in the magnetic sublevels are discussed in [15].

The condensate fraction of the system $\rho^{c} = N^{c}\boldsymbol{\Phi}\boldsymbol{\Phi}^{\dagger}$ is a pure state with $\boldsymbol{k} = \boldsymbol{0}$. Hence, the resulting GP equations that results from minimizing E_{HF}, $\delta E_{HF}/\delta\phi_m^* = 0$, are given by a system of three (nonlinear) equations involving ϕ_m and ρ^{nc}. On the other hand, ρ^{nc} is written as a sum of its eigenvectors $\boldsymbol{\xi}^{\lambda} = (\xi^{\lambda}_{f}, \xi^{\lambda}_{f-1}, \ldots, \xi^{\lambda}_{-f})^{T}$ weighted by its Bose-Einstein distribution factor n_λ,

$$\rho^{nc}_{ij} = \sum_{\lambda} n_\lambda \xi^{\lambda}_{i}\xi^{\lambda *}_{j}, \quad n_\lambda = (e^{\beta\epsilon_\lambda} - 1)^{-1}. \tag{46}$$

The global subindex λ includes the spatial and spinor-quantum numbers, $\lambda = (\boldsymbol{k}, \nu)$, with $\nu = 1, 2, \ldots, 2f+1$ and $\beta = 1/k_B T$, where k_B is the Boltzmann constant. The eigenvectors $\boldsymbol{\xi}^{\lambda}$ and their associated energies ϵ_λ are obtained by the noncondensate Hamiltonian A, given by $A_{ij} = \delta E_{HF}/\delta\rho^{nc}_{ji}$. The decoupling of the spatial and spinor parts in the Hamiltonian A lead to $\epsilon_\lambda = -\hbar^2 k^2/2M + \kappa_\nu$, with κ_ν the eigenvalue of the spinor part of A. In summary, ρ^{nc} is an statistical mixture of thermal atoms with eigenstates labeled by the wave vector $\boldsymbol{k}$, and the index ν that specifies the spinor eigenstate of the HF Hamiltonian A. The spatial part of ρ^{nc} can be integrated using that $\sum_{\boldsymbol{k}} \to (2\pi)^{-3}\int \mathrm{d}\boldsymbol{k}$ [58],

$$\rho^{nc}_{ij} = \sum_{\nu=1}^{2f+1} \xi^{\nu}_{i}\xi^{\nu *}_{j}\Lambda_\nu, \quad \Lambda_\nu = \frac{Li_{3/2}(e^{-\beta\kappa_\nu})}{\lambda^3_{dB}}, \tag{47}$$

where $Li_{3/2}(z)$ is the polylogarithm function and $\lambda_{dB} = h/\sqrt{2\pi M k_B T}$ is the thermal de Broglie wavelength. The eigendecomposition of A_{ij}, which is now a $(2f+1)\times(2f+1)$ matrix, are called the HF equations. The atom fractions N^{c} and N^{nc} can be written in terms of κ_ν because $N^{c} = N - N^{nc}$ and $N^{nc} = \sum_\nu \Lambda_\nu$. Moreover, the A matrix, dependent on ρ^{c} and ρ^{nc}, can also be written in terms of the Λ_ν and then of the κ_ν variables. Finally, we use the fact that A and ρ^{nc} share the same eigenvectors, leading us to obtain a system of algebraic-transcendental equations for the κ_μ eigenenergies of A.

The equations to determine ρ^{c} are still called Gross-Pitaevskii (GP) equations $\delta E_{HF}/\delta\phi_m^* = 0$, and they can be written as $\mu\boldsymbol{\Phi} = L\boldsymbol{\Phi}$, with

$$\begin{aligned} L = c_0(N\mathbb{1}_f + \rho^{nc}) &+ c_1\sum_{\alpha}\{\mathrm{Tr}[F_\alpha\rho]F_\alpha + F_\alpha\rho^{nc}F_\alpha\} \\ &+ \frac{c_2}{5}\mathcal{T}(\rho + \rho^{nc})\mathcal{T}, \end{aligned} \tag{48}$$

where $\alpha = x, y,$ and z. On the other hand, the noncondensate Hamiltonian A, with $A_{ij} = \delta E_{HF}/\delta\rho^{nc}_{ji}$, allows to determine ρ_{nc} with the so-called the Hartree-Fock (HF) equations, and is explicitly given by

$$\begin{aligned} A &= L - \mu\mathbb{1}_5 + c_0\rho^{c} + c_1\sum_{\alpha}F_\alpha\rho^{c}F_\alpha + \frac{c_2}{5}\mathcal{T}\rho^{c}\mathcal{T} \\ &= -\mu\mathbb{1}_5 + c_0(N\mathbb{1}_5 + \rho) \\ &\quad + c_1\sum_{\alpha}\{\mathrm{Tr}[\rho F_\alpha]F_\alpha + F_\alpha\rho F_\alpha\} + \frac{2c_2}{5}\mathcal{T}\rho\mathcal{T}. \end{aligned} \tag{49}$$

The standard procedure is to solve in a self-consistent fashion the GP-HF equations, (48) and (49) [15,17,24]. However, as it is shown below, the symmetries inherited by ρ^{nc} reduce considerably its degrees of freedom and therefore the complexity of the problem. Moreover, the case spin-2 BEC is amenable for the calculation of the associated eigenvectors of each ρ^{nc}, as well as for the derivation of closed equations for the κ_ν energies. In the next section we discuss the calculation of the expressions of κ_ν for low temperatures and analyze the admissible regions of each allowed spin phase. Also, the phase diagrams at finite temperatures can be calculated by finding the ground states defined in terms of the thermodynamic HF potential, $\Phi_{HF} = E_{HF} - TS_{HF}$, where S_{HF} is the HF entropy [18,24].

B. Applications: Admissible regions of the phases

Following the HF approximation, the κ_ν energy is by definition the additional energy that an atom required to be added in ρ^{nc} in the spin state $\boldsymbol{\xi}_\nu$ with order parameter $\boldsymbol{\Phi}$ [18]. Hence,

the energies must satisfy that

$$\kappa_\nu > 0, \tag{50}$$

otherwise the $\mathbf{\Phi}$ phase becomes forbidden and may promote a drastic (quench) evolution to another phase. The condition (50) gives us valuable insights about the regions in which spin phase could exist. In particular, a scenario in which regions of different spinor phases overlap (coexist) can also occur [18]. While the spin phase with the lowest thermodynamic potential gives us the ground phase of the BEC, the others phases give rise to metastable phases [18]. The characterizations of the noncondensate fractions ρ^{nc} presented in the previous sections allow us to calculate the analytical expressions of all the κ_ν energies. In what follows, we discuss how we proceed to calculate the allowed regions in the (c_1, c_2) space, as well as on the physical nature of their boundaries for the case of a spin-2 BEC. For simplicity, we write the equations in a compact form, while the full expressions and details are provided in Appendix C. The new admissible region of each phase, appearing as we increase the temperature (see Fig. 5), includes a region where the phase is metastable [18]. We also obtained that, while for $T = 0$ the whole nematic family is equally valid to be a ground phase, for $T \neq 0$ only the square and polar phases remain as ground states, which are in fact the states with higher point group in the nematic family. This is called in the literature order-by-disorder phenomenon, and it has been predicted for the nematic family of spin-2 BEC in Refs. [59,60].

1. FM case

Let us consider the FM phase of a spin-f BEC, oriented along the z axis [61], and described in general by a state $|f, f\rangle$. The degrees of freedom of a generic noncondensate fraction ρ^{nc} of spin f is $(2f+1)^2$, being 25 in the particular case of $f = 2$. However, exploiting its symmetries, they are reduced to just five for the FM case, which are the Λ_m variables of $\rho^{nc} = \sum_{m=-2}^{2} \Lambda_m |2, m\rangle \langle 2, m|$. Moreover, since the atom fractions N^c and N^{nc} can be written in terms of Λ_m because $N^c = N - N^{nc}$ and $N^{nc} = \sum_m \Lambda_m$, the whole problem has only five unknown variables Λ_m. These variables are functions of the eigenenergies of $A = \delta E_{HF}/\delta \rho^{nc}_{ji}$, κ_m (47). In summary, the eigenvalues of A lead us to a set of equations for the κ_ν energies in terms of a linear combination of the Λ_ν, which are written explicitly in Appendix C. At low temperatures and with $N \sim 10^4$ atoms per cm^3, which is a typical value in the experiments, the terms in the energies κ_ν proportional to N become the dominant terms, defining the physical boundaries of the allowed regions. For the FM phase, such boundaries are constrained by the conditions (see Fig. 5), where

$$\begin{aligned} \kappa_{-1}^{(FM)} &= -6c_1 N + \mathcal{O}(\Lambda_\nu) = 0, \\ \kappa_{-2}^{(FM)} &= 2N\left(-4c_1 + \frac{c_2}{5}\right) + \mathcal{O}(\Lambda_\nu) = 0, \end{aligned} \tag{51}$$

where we have added the spin-phase name of the eigenenergy as a superindex. We can observe that when $T = 0$, and then $\Lambda_\nu = 0$, the conditions (51) are identical to the phase transitions in the MF approximation. Consequently, the FM phase is only defined in the regions where is the ground state, i.e., it is not a metastable phase anywhere at $T = 0$. We plot the

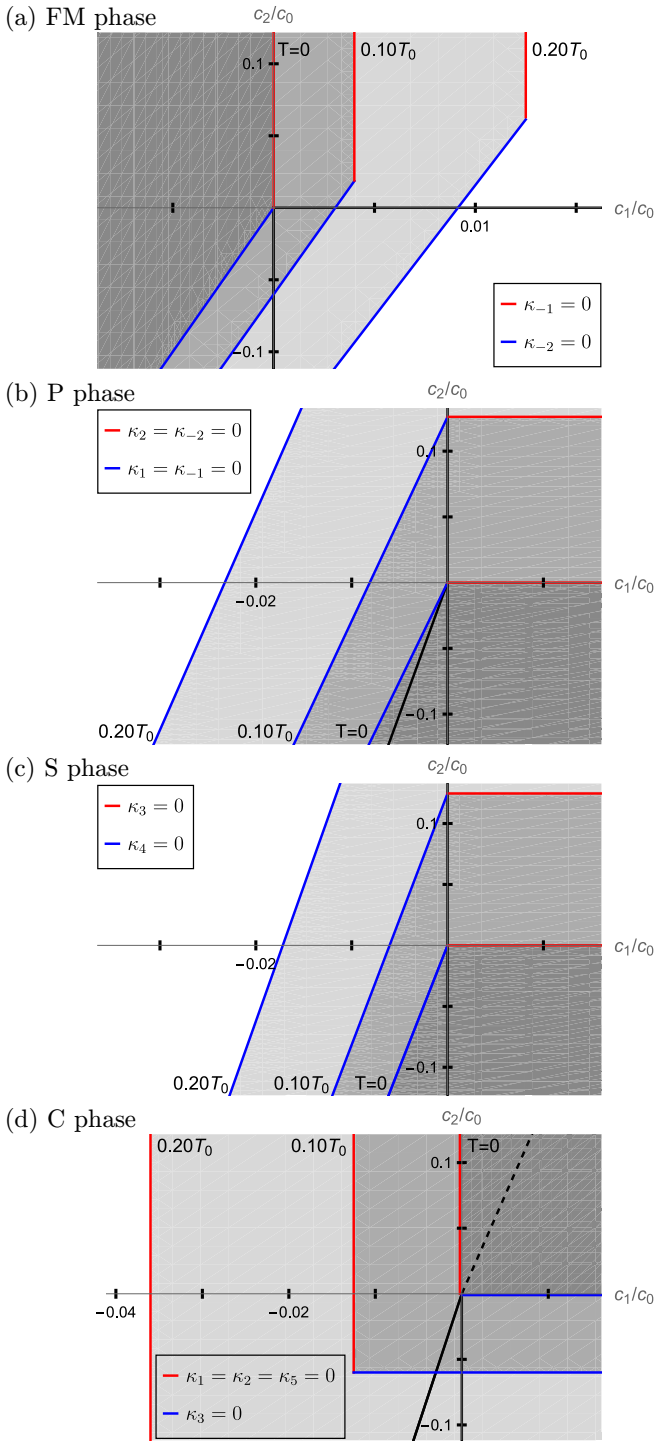

FIG. 5. (a) Allowed region of the FM spin-2 BEC phase in the (c_1, c_2) parameter space at $T/T_0 = 0, 0.1, 0.2$ colored in gray scale (from dark to light), respectively, where T_0 is the condensation temperature of an ideal scalar gas (12). The boundaries (red and blue lines) are defined by the conditions (51), where we omit the superindex of the κ_ν eigenenergies. The black solid lines are the ground-phase boundaries of the other spin phases at $T = 0$ (see Fig. 1). Similar graphics are shown below for the (b) P, (c) S, and (d) C phases, with boundaries defined by Eqs. (52), (53), and (55), respectively. The dashed line in caption (d) corresponds to the (c_1, c_2) values, where ρ^{nc} has a fourth-degenerated eigenvalue.

allowed regions of the FM phase, and the other phases, for the finite temperatures $T/T_0 = 0, 0.1, 0.2$ calculated numerically in Fig. 5, which agrees with the previous discussion. The phase transitions of the FM phase do not depend on the temperature. On the other hand, its allowed region increases with respect to the temperature, which would be the (c_1, c_2) values where the FM phase could be metastable.

2. P phase

The P phase is equal to the $|2, 0\rangle$ phase, which has the same symmetries as the FM phase plus the time-reversal symmetry. Hence, besides to have the same density matrix as the FM phase, $\rho^{nc} = \sum_{m=-2}^{2} \Lambda_m |2, m\rangle \langle 2, m|$, the additional symmetry yields $\Lambda_2 = \Lambda_{-2}$ and $\Lambda_1 = \Lambda_{-1}$. The allowed region of P at finite temperatures (see Fig. 5) is restricted by the conditions

$$\kappa_2^{(P)} = \kappa_{-2}^{(P)} = -\frac{c_2}{5}N + \mathcal{O}(\Lambda_\nu) = 0,$$
$$\kappa_1^{(P)} = \kappa_{-1}^{(P)} = \left(3c_1 - \frac{c_2}{5}\right)N + \mathcal{O}(\Lambda_\nu) = 0. \quad (52)$$

The left-lower bound does not coincide to the $P - S$ transition phase even at all temperatures, implying that the P phase is metastable over the ground-phase region of the S phase even at $T = 0$.

3. S phase

The allowed region of the S phase coincides to the zone where the nematic family is the ground phase at $T = 0$. The left-lower and upper boundaries are given as

$$\kappa_3^{(S)} = -\frac{c_2}{5}N + \mathcal{O}(\Lambda_\nu) = 0,$$
$$\kappa_4^{(S)} = \left(4c_1 - \frac{c_2}{5}\right)N + \mathcal{O}(\Lambda_\nu) = 0, \quad (53)$$

with corresponding spin states given by Eqs. (36) and (37),

$$\boldsymbol{v}_3 = (0, 0, 1, 0, 0)^{\mathrm{T}}, \quad \boldsymbol{v}_4 = (-1, 0, 0, 0, 1)^{\mathrm{T}}/\sqrt{2}. \quad (54)$$

4. C case

We plot in Fig. 5 the allowed regions at finite temperatures of the C phase. The left and lower boundaries are associated to the $\kappa_1^{(C)}, \kappa_3^{(C)} = 0$ conditions, respectively, where

$$\kappa_1^{(C)} = \kappa_2^{(C)} = \kappa_5^{(C)} = 2c_1 N + \mathcal{O}(\Lambda_\nu) = 0,$$
$$\kappa_3^{(C)} = \frac{2c_2}{5}N + \mathcal{O}(\Lambda_\nu) = 0. \quad (55)$$

The numerical calculations show the predicted triple degeneracy of ρ^{nc} over its allowed region. Moreover, the spectrum of ρ^{nc} is fourth degenerated over the line $c_2 = 5c_1$. This result can be explained by the previous equations, where κ_1 and κ_3 are functionally equal when we substitute the conditions $c_2 = 5c_1$ and $\Lambda_1 = \Lambda_3$.

V. CONCLUSIONS

We have studied the emergent physics occurring in the spin phases of BECs with point-group symmetries. By exploiting the condition that HF theory preserves self-consistent symmetries, we developed a method based in the Majorana representation of mixed states to completely characterize the noncondensate fraction of atoms through minimum degrees of freedom required for the full characterization of a given point-group symmetry. Such characterizations can be applied to any model with self-consistent symmetries even at finite temperatures. In particular, we use them to review the multipolar magnetic moments of two families of spin phases, called the $|f, m\rangle$ and NOON phases, respectively. We also apply it to study some exotic phases associated with certain platonic solids and that are known to support non-Abelian topological excitations. In addition, we presented a systematic study of the behavior of the phase boundaries of spin-2 BECs as a function of the temperature. This method can be generalized to investigate spin BEC phases in more complex scenarios. As such, the only prerequisite is the existence of phases characterized with a high-symmetry group, and that the application of perturbation theory still keeps self-consistent symmetries. For instance, it can be straightforwardly implemented for any confinement trap. The approach can be also be extended to study the spin phases in BEC systems in which the spatial and spinorial parts of its wave function are no longer separable, as occurs when we consider dipolar interactions [62], synthetic spin-orbit coupling [63], or the dynamics of BEC spin phases via time-dependent variations [64].

ACKNOWLEDGMENTS

E.S.-E. acknowledges support from the postdoctoral fellowships offered by the DGAPA-UNAM and the IPD-STEMA programs of the University of Liège. F.M. acknowledges the support of DGAPA-UNAM through Projects No. PAPIIT and No. IN113920.

APPENDIX A: CHARACTERIZATION OF THE GLOBAL PHASE FACTORS IN THE MAJORANA REPRESENTATION FOR MIXED STATES

The constellations plotted in Fig. 4 on the sphere of different radii characterize the density matrix of the noncondensate fraction up to the global phase factor of the $\boldsymbol{\rho}_\sigma$ vectors. However, one can associate the global phase factor of $\boldsymbol{\rho}_\sigma$ to an equivalence class of the set of half the points in the constellation. All the details about this characterization are given in Ref. [45]. Here we explain the basic notions and the schematic procedure. Let us consider a vector $\boldsymbol{\rho}_\sigma$ of the Majorana representation of a mixed state ρ, which we write as a ket $|\boldsymbol{\rho}_\sigma\rangle$ to simplify the discussion. The state $|\boldsymbol{\rho}_\sigma\rangle$ has a Majorana constellation $\mathcal{C}_\sigma$ with 2σ stars denoted by the tuple of unit vectors $(\upsilon_1, \ldots, \upsilon_{2\sigma})$. The constellation $\mathcal{C}_{\rho_\sigma}$ has antipodal symmetry, which implies that there exist subconstellations of σ stars $\boldsymbol{c} = (\boldsymbol{v}_{\alpha_1}, \ldots, \boldsymbol{v}_{\alpha_\sigma})$ such that

$$\{\boldsymbol{c}\} \cup \{-\boldsymbol{c}\} = \mathcal{C}_{\rho_\sigma}, \quad (A1)$$

with $-\boldsymbol{c} = (-\boldsymbol{v}_{\alpha_1}, \ldots, -\boldsymbol{v}_{\alpha_\sigma})$. In general, $\{\boldsymbol{c}\}$ is not unique, and the other choices can be written with respect to $\boldsymbol{c}$ inverting the direction of some of its stars $\boldsymbol{\gamma c} \equiv (\gamma_1 \boldsymbol{v}_1, \ldots, \gamma_\sigma \boldsymbol{v}_\sigma)$, with $\gamma_\alpha = 1$ or -1. Now we can define a spin-$\sigma/2$ state $|z_c\rangle$ for each $\boldsymbol{c}$ via the Majorana representation. Analogously, the antipodal tuple $-\boldsymbol{c}$ has associated a spin-$\sigma/2$ state that we denote by $|z_c^{\mathcal{T}}\rangle \equiv \mathcal{T}|z_c\rangle$ and it is completely defined by the

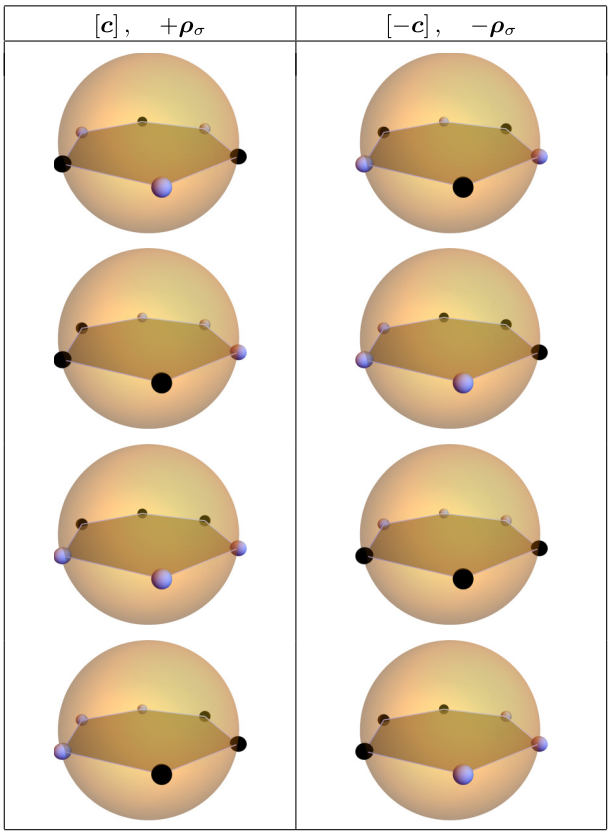

FIG. 6. The two equivalence classes $[\pm\boldsymbol{c}]$ of the constellations associated to the Majorana stars of a hexagon. Each class is associated to the global sign of the vector $\pm\boldsymbol{\rho}_3$.

components of $|z\rangle$:

$$\mathcal{T}\,|z_c\rangle = \sum_m (-1)^{f+m} t^*_{-m}\,|f,m\rangle\,, \quad \text{for } |z_c\rangle = \sum_m t_m\,|f,m\rangle\,. \tag{A2}$$

Both states define a σ-spin state, denoted by $|Z_c\rangle$, by its tensor product projected on the totally symmetric subspace

$$|Z_c\rangle = A\mathcal{P}_\sigma\big(\,|z_c\rangle \otimes \big|z_c^{\mathcal{T}}\big\rangle\big), \quad \text{with } \mathcal{P}_\sigma = \sum_m |\sigma,m\rangle\,\langle\sigma,m|\,, \tag{A3}$$

where A is a positive normalization factor. Surprisingly, $|Z_c\rangle$ is independent of the global phase factor of $|z_c\rangle$ [45]. Moreover, $|Z_c\rangle$ is equal to one of the possible options $\pm\,|\boldsymbol{\rho}_\sigma\rangle$. Hence, we can associate to each choice of $\pm\,|\boldsymbol{\rho}_\sigma\rangle$, all the tuples $\boldsymbol{c}$ of σ stars that define the same spin state $\pm\,|\boldsymbol{\rho}_\sigma\rangle$ with the latter procedure. It turns out that the tuples $\boldsymbol{c}$ that define $|Z_c\rangle = |\boldsymbol{\rho}_\sigma\rangle$ differ among themselves only by an even number of stars [45]. We then can define two equivalence classes between the subconstellations that satisfy Eq. (A1):

$$\left\{\boldsymbol{\gamma c} \subset \mathcal{C}^{(\sigma)} | \gamma_k = 1 \text{ or } -1 \text{ and } \prod_{k=1}^{\sigma}\gamma_k = +1\right\},$$
$$\left\{\boldsymbol{\gamma c} \subset \mathcal{C}^{(\sigma)} | \gamma_k = 1 \text{ or } -1 \text{ and } \prod_{k=1}^{\sigma}\gamma_k = -1\right\}. \tag{A4}$$

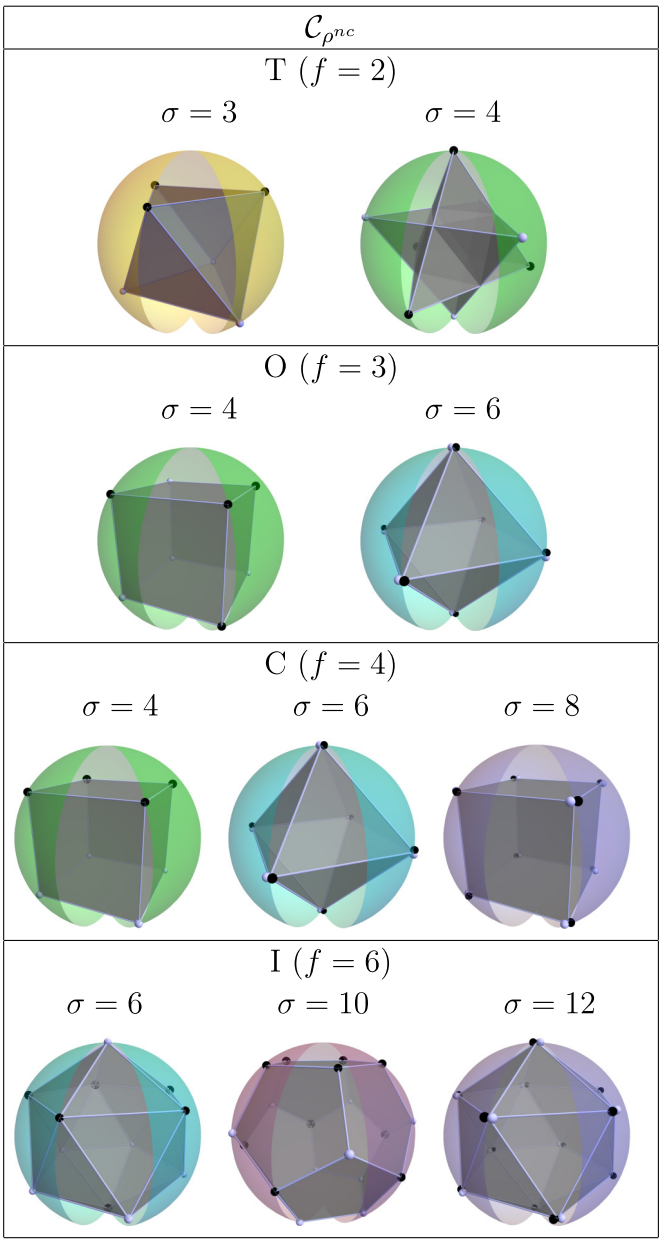

FIG. 7. Majorana representation of the noncondensate fractions ρ^{nc} associated to the platonic phases of the spinor BEC. The set of black stars constitutes a representative element of the equivalence class $[\boldsymbol{c}]$ of $\boldsymbol{\rho}_\sigma$.

Any element of any class produces the same spin state $|\rho_\sigma\rangle$ with Eq. (A3) up to a global sign. On the other hand, only elements of the same class produce the same vector $\boldsymbol{\rho}_\sigma$, i.e., the same state and the same phase factor of $\boldsymbol{\rho}_\sigma$. To exemplify the method mentioned above, let us calculate the equivalence class associated to a vector $\boldsymbol{\rho}_3$ with

$$\rho_{3m} = (\delta_{m,3} + \delta_{m,-3})/\sqrt{2}. \tag{A5}$$

Its Majorana constellation consists of six points that conform a regular hexagon on the equator (see Fig. 6). Now, a tuple of stars $\boldsymbol{c}$ that satisfies Eq. (A1) consists of three points, let us say the black points of the first image of Fig. 6, which is

associated to a spin-3/2 state equal to

$$|z_c\rangle = \frac{e^{i\beta}}{\sqrt{2}}\left(\left|\frac{3}{2},\frac{3}{2}\right\rangle + \left|\frac{3}{2},-\frac{3}{2}\right\rangle\right), \tag{A6}$$

where $e^{i\beta}$ is a general global phase factor. The antipodal state is given by Eq. (A2),

$$|z_c^{\mathcal{T}}\rangle = \frac{e^{-i\beta}}{\sqrt{2}}\left(\left|\frac{3}{2},-\frac{3}{2}\right\rangle - \left|\frac{3}{2},\frac{3}{2}\right\rangle\right), \tag{A7}$$

and the respective spin-3 state $|Z_c\rangle$ associated to the tuple $\boldsymbol{c}$ is calculated using Eq. (A3),

$$\begin{aligned}|z_c\rangle \otimes |z_c^{\mathcal{T}}\rangle = \frac{1}{2}\Bigg(&\left|\frac{3}{2},-\frac{3}{2}\right\rangle \otimes \left|\frac{3}{2},-\frac{3}{2}\right\rangle - \left|\frac{3}{2},\frac{3}{2}\right\rangle \otimes \left|\frac{3}{2},\frac{3}{2}\right\rangle \\ &+ \left|\frac{3}{2},\frac{3}{2}\right\rangle \otimes \left|\frac{3}{2},-\frac{3}{2}\right\rangle - \left|\frac{3}{2},\frac{3}{2}\right\rangle \otimes \left|\frac{3}{2},-\frac{3}{2}\right\rangle\Bigg)\end{aligned}$$

$$|Z_c\rangle = \frac{1}{\sqrt{2}}(|3,3\rangle + |3,-3\rangle), \tag{A8}$$

where we use the basis transformation between coupled and decoupled angular momentum states of spin 3/2. Therefore the tuple $\boldsymbol{c}$ gives the same $\boldsymbol{\rho}_3$ given in Eq. (A5), and then its equivalence class is given by all the constellations of three points that differ from $\boldsymbol{c}$ by an even numbers of stars. All the possible cases are plotted in Fig. 6. We also include in the figure the other equivalence class $[-\boldsymbol{c}]$ which, by a similar calculation as in Eq. (A8), gives the vector $-\boldsymbol{\rho}_3$.

In summary, a complete characterization of a mixed state is the collection of $2f$ constellations, each one on a sphere of radii r_σ and with one of the two possible equivalence classes $[\pm\boldsymbol{c}]$ (A4), with $\boldsymbol{c}$ a representative element. We plot in Fig. 7 the examples of the complete characterization of the general mixed states with a symmetry associated to a platonic solid shown in Fig. 4. We use the vectors $\boldsymbol{\rho}_\sigma$ mentioned in the main text Eqs. (38), (41)–(44) and we assume that $r_\sigma \geqslant 0$. We indicate a representative element of each equivalence class with the black stars.

APPENDIX B: QUADRUPOLAR MAGNETIC MOMENT IN TERMS OF THE TENSOR OPERATORS

In this Appendix we calculate the components $N_{\nu_1\nu_2}$ by using Eqs. (26)–(29),

$$N_{zz} = w^2 T_{10}^2 = w^2 \sum_{l,m} \chi(1,1,l,f) c_{10,10}^{lm} T_{1m} = \frac{1}{30}\left(10f(f+1)\sqrt{2f+1}T_{00} + \sqrt{5\frac{(2f+3)!}{(2f-2)!}}T_{20}\right), \tag{B1}$$

$$\begin{aligned}N_{xx} &= \frac{w^2}{2}\left[-\frac{2}{\sqrt{3}}\chi(1,1,0,f)T_{00} + \chi(1,1,2,f)\left(T_{22}+T_{2-2}-\sqrt{\frac{2}{3}}T_{20}\right)\right] \\ &= \frac{f(f+1)\sqrt{2f+1}}{3}T_{00} + \frac{1}{4\sqrt{30}}\sqrt{\frac{(2f+3)!}{(2f-2)!}}\left(T_{22}+T_{2-2}-\sqrt{\frac{2}{3}}T_{20}\right),\end{aligned} \tag{B2}$$

$$N_{yy} = \frac{f(f+1)\sqrt{2f+1}}{3}T_{00} - \frac{1}{4\sqrt{30}}\sqrt{\frac{(2f+3)!}{(2f-2)!}}\left(T_{22}+T_{2-2}+\sqrt{\frac{2}{3}}T_{20}\right), \tag{B3}$$

$$N_{xz} = N_{zx} = \frac{w^2}{2}\chi(1,1,2,f)(T_{2-1}-T_{21}) = \frac{4}{\sqrt{30}}\sqrt{\frac{(2f+3)!}{(2f-2)!}}(T_{2-1}-T_{21}), \tag{B4}$$

$$N_{yz} = N_{zy} = \frac{iw^2}{2}\chi(1,1,2,f)(T_{2-1}+T_{21}) = \frac{4i}{\sqrt{30}}\sqrt{\frac{(2f+3)!}{(2f-2)!}}(T_{2-1}+T_{21}), \tag{B5}$$

$$N_{xy} = N_{yx} = \frac{iw^2\chi(1,1,2,f)}{2}(T_{2-2}-T_{22}) = \frac{i}{4\sqrt{30}}\sqrt{\frac{(2f+3)!}{(2f-2)!}}(T_{2-2}-T_{22}). \tag{B6}$$

APPENDIX C: FULL EXPRESSION OF THE κ_ν ENERGIES AND THE CHEMICAL POTENTIAL OF THE PHASES OF SPIN-2 BEC

We enlist the chemical potential and the κ_ν energies following the same notation as in the main text.

1. FM case

$$\mu^{(FM)} = c_0(N+\Lambda_2) + 2c_1(2N+2\Lambda_2-2\Lambda_0-3\Lambda_{-1}-4\Lambda_{-2}) + \frac{2c_2\Lambda_{-2}}{5},$$

$$\kappa_2^{(FM)} = (c_0+4c_1)N^c,$$

$$\kappa_1^{(FM)} = c_0(\Lambda_1 - \Lambda_2) + c_1(-4\Lambda_2 - 2\Lambda_1 + 3\Lambda_0 + \Lambda_{-1} + 2\Lambda_{-2}) + \frac{2c_2}{5}(\Lambda_{-1} - \Lambda_{-2}),$$
$$\kappa_0^{(FM)} = c_0(\Lambda_0 - \Lambda_2) + c_1(-4N - 4\Lambda_2 + 3\Lambda_1 + 4\Lambda_0 + 9\Lambda_{-1} + 8\Lambda_{-2}) + \frac{2c_2}{5}(\Lambda_0 - \Lambda_{-2}),$$
$$\kappa_{-1}^{(FM)} = c_0(\Lambda_{-1} - \Lambda_2) + c_1(-6N - 4\Lambda_2 + \Lambda_1 + 9\Lambda_0 + 10\Lambda_{-1} + 14\Lambda_{-2}) + \frac{2c_2}{5}(\Lambda_1 - \Lambda_{-2}),$$
$$\kappa_{-2}^{(FM)} = c_0(\Lambda_{-2} - \Lambda_2) + 2c_1(-4N - 2\Lambda_2 + \Lambda_1 + 4\Lambda_0 + 7\Lambda_{-1} + 10\Lambda_{-2}) + \frac{2c_2}{5}(N - \Lambda_1 - \Lambda_0 - \Lambda_{-1} - 2\Lambda_{-2}). \quad \text{(C1)}$$

2. P phase

$$\mu^{(P)} = c_0(N + \Lambda_0) + 6c_1\Lambda_1 + \frac{c_2}{5}(N + \Lambda_0 - 2\Lambda_1 - 2\Lambda_2),$$
$$\kappa_2^{(P)} = \kappa_{-2}^{(P)} = c_0(\Lambda_2 - \Lambda_0) + 4c_1(\Lambda_2 - \Lambda_1) - \frac{c_2}{5}(N + \Lambda_0 - 2\Lambda_1 - 4\Lambda_2),$$
$$\kappa_1^{(P)} = \kappa_{-1}^{(P)} = c_0(\Lambda_1 - \Lambda_0) + c_1(3N - 11\Lambda_1 - 4\Lambda_2) - \frac{c_2}{5}(N + \Lambda_0 - 4\Lambda_1 - 2\Lambda_2),$$
$$\kappa_0^{(P)} = \left(\frac{c_2 + 5c_0}{5}\right)N^c. \quad \text{(C2)}$$

3. S phase

$$\mu^{(S)} = c_0(N + \Lambda_5) + 2c_1(\Lambda_2 + 2\Lambda_4) + \frac{c_2}{5}(N - 2\Lambda_2 - \Lambda_3 - \Lambda_4 + \Lambda_5),$$
$$\kappa_1^{(S)} = \kappa_2^{(S)} = +c_0(\Lambda_2 - \Lambda_5) + c_1(N - 3\Lambda_2 + 2\Lambda_3 - 4\Lambda_4) + \frac{c_2}{5}(-N + 4\Lambda_2 + \Lambda_3 + \Lambda_4 - \Lambda_5),$$
$$\kappa_3^{(S)} = c_0(\Lambda_3 - \Lambda_5) + 4c_1(\Lambda_2 - \Lambda_4) + \frac{c_2}{5}(-N + 2\Lambda_2 + 3\Lambda_3 + \Lambda_4 - \Lambda_5),$$
$$\kappa_4^{(S)} = c_0(\Lambda_4 - \Lambda_5) - 4c_1(-N + 2\Lambda_2 + \Lambda_3 + 2\Lambda_4) + \frac{c_2}{5}(-N + 2\Lambda_2 + \Lambda_3 + 3\Lambda_4 - \Lambda_5),$$
$$\kappa_5^{(S)} = \frac{(5c_0 + c_2)}{5}N^c. \quad \text{(C3)}$$

4. C case

The chemical potential is equal to

$$\mu^{(C)} = c_0(N + \Lambda_4) + 6c_1\Lambda_1 + \frac{2c_2}{5}\Lambda_3. \quad \text{(C4)}$$

After we write ρ^{nc} in terms of the Λ_ν, we can now calculate the HF equations given by the eigenvalues and eigenvectors equal to Eq. (49),

$$\kappa_1^{(C)} = \kappa_2^{(C)} = \kappa_5^{(C)} = c_0(\Lambda_1 - \Lambda_4) + 2c_1(N - 5\Lambda_1) + \frac{2c_2}{5}(\Lambda_1 - \Lambda_3),$$
$$\kappa_3^{(C)} = c_0(\Lambda_3 - \Lambda_4) + \frac{2c_2}{5}(N - 3\Lambda_1 - 2\Lambda_3),$$
$$\kappa_4^{(C)} = c_0N^c. \quad \text{(C5)}$$

[1] P. W. Dieter Vollhardt, *The Superfluid Phases of Helium 3*, 1st ed. (Taylor & Francis, London, 1990).

[2] S. Kruchinin, H. Nagao, and S. Aono, *Modern Aspects of Superconductivity - Theory of Superconductivity* (World Scientific, Singapore, 2011).

[3] M. Lewenstein, A. Sanpera, and V. Ahufinger, *Ultracold Atoms in Optical Lattices: Simulating Quantum Many-Body Systems* (Oxford University Press, London, 2012).

[4] Y. Kawaguchi and M. Ueda, Phys. Rep. **520**, 253 (2012).

[5] H. Schmaljohann, M. Erhard, J. Kronjäger, M. Kottke, S. van Staa, L. Cacciapuoti, J. J. Arlt, K. Bongs, and K. Sengstock, Phys. Rev. Lett. **92**, 040402 (2004).

[6] B. Naylor, M. Brewczyk, M. Gajda, O. Gorceix, E. Marechal, L. Vernac, and B. Laburthe-Tolra, Phys. Rev. Lett. **117**, 185302 (2016).

[7] C. Frapolli, T. Zibold, A. Invernizzi, K. Jiménez-García, J. Dalibard, and F. Gerbier, Phys. Rev. Lett. **119**, 050404 (2017).

[8] K. Jiménez-García, A. Invernizzi, B. Evrard, C. Frapolli, J. Dalibard, and F. Gerbier, Nat. Commun. **10**, 1422 (2019).

[9] J. Stenger, S. Inouye, D. Stamper-Kurn, H.-J. Miesner, A. Chikkatur, and W. Ketterle, Nature (London) **396**, 345 (1998).

[10] M.-S. Chang, C. D. Hamley, M. D. Barrett, J. A. Sauer, K. M. Fortier, W. Zhang, L. You, and M. S. Chapman, Phys. Rev. Lett. **92**, 140403 (2004).

[11] Q. Beaufils, R. Chicireanu, T. Zanon, B. Laburthe-Tolra, E. Maréchal, L. Vernac, J.-C. Keller, and O. Gorceix, Phys. Rev. A **77**, 061601(R) (2008).

[12] T. Weber, J. Herbig, M. Mark, H.-C. Nägerl, and R. Grimm, Science **299**, 232 (2003).

[13] M. Lu, N. Q. Burdick, S. H. Youn, and B. L. Lev, Phys. Rev. Lett. **107**, 190401 (2011).

[14] K. Aikawa, A. Frisch, M. Mark, S. Baier, A. Rietzler, R. Grimm, and F. Ferlaino, Phys. Rev. Lett. **108**, 210401 (2012).

[15] Y. Kawaguchi, N. T. Phuc, and P. B. Blakie, Phys. Rev. A **85**, 053611 (2012).

[16] B. Pasquiou, E. Maréchal, L. Vernac, O. Gorceix, and B. Laburthe-Tolra, Phys. Rev. Lett. **108**, 045307 (2012).

[17] A. Griffin, T. Nikuni, and E. Zaremba, *Bose-Condensed Gases at Finite Temperatures* (Cambridge University Press, Cambridge, England, 2009).

[18] E. Serrano-Ensástiga and F. Mireles, Phys. Rev. A **104**, 063308 (2021).

[19] M. Matuszewski, T. J. Alexander, and Y. S. Kivshar, Phys. Rev. A **78**, 023632 (2008).

[20] D. M. Stamper-Kurn, H.-J. Miesner, A. P. Chikkatur, S. Inouye, J. Stenger, and W. Ketterle, Phys. Rev. Lett. **83**, 661 (1999).

[21] M. Sadgrove, Y. Eto, S. Sekine, H. Suzuki, and T. Hirano, J. Phys. Soc. Jpn. **82**, 094002 (2013).

[22] H.-X. Yang, T. Tian, Y.-B. Yang, L.-Y. Qiu, H.-Y. Liang, A.-J. Chu, C. B. Dağ, Y. Xu, Y. Liu, and L.-M. Duan, Phys. Rev. A **100**, 013622 (2019).

[23] J. H. Kim, D. Hong, S. Kang, and Y. Shin, Phys. Rev. A **99**, 023606 (2019).

[24] J.-P. Blaizot and G. Ripka, *Quantum Theory of Finite Systems* (MIT Press Cambridge, MA, 1986).

[25] R. Barnett, A. Turner, and E. Demler, Phys. Rev. Lett. **97**, 180412 (2006).

[26] H. Mäkelä and K.-A. Suominen, Phys. Rev. Lett. **99**, 190408 (2007).

[27] Y. Kawaguchi and M. Ueda, Phys. Rev. A **84**, 053616 (2011).

[28] T. Tian, H.-X. Yang, L.-Y. Qiu, H.-Y. Liang, Y.-B. Yang, Y. Xu, and L.-M. Duan, Phys. Rev. Lett. **124**, 043001 (2020).

[29] E. Majorana, Nuovo Cimento **9**, 43 (1932).

[30] K. Kasamatsu, M. Tsubota, and M. Ueda, Int. J. Mod. Phys. B **19**, 1835 (2005).

[31] M. Kobayashi, Y. Kawaguchi, M. Nitta, and M. Ueda, Phys. Rev. Lett. **103**, 115301 (2009).

[32] C. V. Ciobanu, S.-K. Yip, and T.-L. Ho, Phys. Rev. A **61**, 033607 (2000).

[33] T. P. Meyrath, F. Schreck, J. L. Hanssen, C.-S. Chuu, and M. G. Raizen, Phys. Rev. A **71**, 041604(R) (2005).

[34] C. J. Pethick and H. Smith, *Bose-Einstein Condensation in Dilute Gases* (Cambridge University Press, Cambridge, England, 2008).

[35] S.-K. Yip, Phys. Rev. A **75**, 023625 (2007).

[36] L. Michel, Rev. Mod. Phys. **52**, 617 (1980).

[37] I. Bengtsson and K. Życzkowski, *Geometry of Quantum States: An Introduction to Quantum Entanglement* (Cambridge University Press, Cambridge, England, 2017).

[38] C. Chryssomalakos, E. Guzmán-González, and E. Serrano-Ensástiga, J. Phys. A: Math. Theor. **51**, 165202 (2018).

[39] C. Bradley and A. Cracknell, *The Mathematical Theory of Symmetry in Solids: Representation Theory for Point Groups and Space Groups* (Oxford University Press, Oxford, England, 2010).

[40] M. Ueda and M. Koashi, Phys. Rev. A **65**, 063602 (2002).

[41] N. D. Mermin, Phys. Rev. A **9**, 868 (1974).

[42] N. T. Phuc, Y. Kawaguchi, and M. Ueda, Ann. Phys. **328**, 158 (2013).

[43] A. Griffin, Phys. Rev. B **53**, 9341 (1996).

[44] D. M. Stamper-Kurn, M. R. Andrews, A. P. Chikkatur, S. Inouye, H.-J. Miesner, J. Stenger, and W. Ketterle, Phys. Rev. Lett. **80**, 2027 (1998).

[45] E. Serrano-Ensástiga and D. Braun, Phys. Rev. A **101**, 022332 (2020).

[46] U. Fano, Phys. Rev. **90**, 577 (1953).

[47] D. Brink and G. Satchler, *Theory of Angular Momentum* (Clarendon Press, Oxford, 1968).

[48] D. Varshalovich, A. Moskalev, and V. Khersonskii, *Quantum Theory of Angular Momentum* (World Scientific, Singapore, 1988).

[49] J. Zimba, Electro. J. Theo. Phys. **3**, 143 (2006).

[50] O. Giraud, D. Braun, D. Baguette, T. Bastin, and J. Martin, Phys. Rev. Lett. **114**, 080401 (2015).

[51] D. Baguette, T. Bastin, and J. Martin, Phys. Rev. A **90**, 032314 (2014).

[52] D. Baguette, F. Damanet, O. Giraud, and J. Martin, Phys. Rev. A **92**, 052333 (2015).

[53] C. Chryssomalakos and H. Hernández-Coronado, Phys. Rev. A **95**, 052125 (2017).

[54] F. Bouchard, P. de la Hoz, G. Björk, R. W. Boyd, M. Grassl, Z. Hradil, E. Karimi, A. B. Klimov, G. Leuchs, J. Řeháček, and L. L. Sánchez-Soto, Optica **4**, 1429 (2017).

[55] J. Martin, S. Weigert, and O. Giraud, Quantum **4**, 285 (2020).

[56] G. S. Agarwal, *Quantum Optics* (Cambridge University Press, Cambridge, England, 2012).

[57] D. Baguette and J. Martin, Phys. Rev. A **96**, 032304 (2017).

[58] The full spatial density matrix of ρ^{nc} includes its off-diagonal terms $\langle\delta^\dagger(\boldsymbol{r}_1)\delta(\boldsymbol{r}_2)\rangle$. However, since we are only interested in the spinorial sector, we integrate over the space, and only the diagonal terms contribute in Eq. (47).

[59] A. M. Turner, R. Barnett, E. Demler, and A. Vishwanath, Phys. Rev. Lett. **98**, 190404 (2007).
[60] J. L. Song, G. W. Semenoff, and F. Zhou, Phys. Rev. Lett. **98**, 160408 (2007).
[61] This could be achieved by a process of constant magnetization about the z axis and then turning the fields off $p = q = 0$.
[62] T. Lahaye, C. Menotti, L. Santos, M. Lewenstein, and T. Pfau, Rep. Prog. Phys. **72**, 126401 (2009).
[63] Y.-J. Lin, K. Jiménez-García, and I. B. Spielman, Nature (London) **471**, 83 (2011).
[64] V. M. Pérez-García, H. Michinel, J. I. Cirac, M. Lewenstein, and P. Zoller, Phys. Rev. Lett. **77**, 5320 (1996).